



Cite this: *Environ. Sci.: Atmos.*, 2025, 5, 242

Highly diverse emission of volatile organic compounds by Sitka spruce and determination of their emission pathways†

Hayley Furnell,^{ab} John Wenger,^{ID ab} Astrid Wingler,^{bc} Kieran N. Kilcawley,^{de} David T. Mannion,^{de} Iwona Skibinska^{de} and Julien Kammer^{ID *abf}

The diversity of biogenic volatile organic compounds (BVOCs) emitted by Sitka spruce (*Picea sitchensis*) saplings, housed in a plant growth chamber, has been investigated using a combination of on-line (time-of-flight chemical ionisation mass spectrometry) and off-line (gas chromatography-mass spectrometry) measurement techniques. In total, 74 BVOCs were identified in the Sitka spruce emissions, considerably more than reported previously. Among the emitted BVOCs, 52 were oxygenated compounds, with piperitone ($C_{10}H_{16}O$), an oxygenated monoterpene, being the most abundant. Other prevalent emissions included isoprene, five monoterpenes (myrcene, β -phellandrene, δ -limonene, α -pinene, and camphene), cinnamaldehyde and camphor. Temperature and photosynthetic photon flux density (PPFD) were found to be the main drivers of emissions, with BVOCs exhibiting a range of responses to these factors. Three different plant growth cycles were used to identify the emission pathways (pooled or biosynthetic) for each BVOC, through determination of the relationships of the emission flux with temperature and with PPFD. During these cycles, all BVOCs showed clear diurnal patterns that were highly reproducible during consecutive days. The majority of the BVOCs emitted by Sitka spruce were found to originate from biosynthetic and pooled pathways simultaneously, with those from one sapling having a much lower contribution from the biosynthetic pathway. Standardised emission fluxes (temperature 30 °C and PPFD 1000 $\mu\text{mol m}^{-2} \text{s}^{-1}$) were calculated for all BVOCs using the appropriate standardisation model (pooled, biosynthetic or combined). Standard emission factors were calculated to be 17.29 $\mu\text{g g}_{\text{dw}}^{-1} \text{h}^{-1}$ for piperitone, 6.3 $\mu\text{g g}_{\text{dw}}^{-1} \text{h}^{-1}$ for isoprene and 0.93 $\mu\text{g g}_{\text{dw}}^{-1} \text{h}^{-1}$ for monoterpenes, indicating that Sitka spruce is a strong BVOC emitter.

Received 10th October 2024
 Accepted 20th December 2024

DOI: 10.1039/d4ea00138a
rsc.li/esatmospheres

Environmental significance

The paper investigated biogenic volatile organic compounds (BVOCs) emitted by Sitka spruce (*Picea sitchensis*), one of the most commonly planted trees in North Western Europe. 74 BVOCs were identified, 52 of which were oxygenated compounds. For the first time, piperitone ($C_{10}H_{16}O$) has been identified as the dominant BVOC emitted by Sitka spruce. Temperature and solar radiation were found to be the main drivers of emissions. The contribution of emission pathways (pooled or biosynthetic) was evaluated for each BVOC. Surprisingly, most of BVOCs were found to originate from both biosynthetic and pooled pathways simultaneously. Standardised emissions were calculated for all BVOCs showing that Sitka spruce is a strong BVOC emitter, meaning that large scale Sitka spruce plantations may significantly affect local air quality.

1. Introduction

Sitka spruce (*Picea sitchensis*) is native to the west coast of North America¹ and due to its rapid growth in maritime climates with moist soils, it is commonly used in forestry plantations in north-western Europe. For example, Sitka spruce accounts for over 50% of forestry by area in Ireland² and over 26% in the UK.³ Forestry plantations have environmental impacts on the local area, influencing both biodiversity^{4,5} and climate.^{6,7} Each different plant species emits a unique mixture of biogenic volatile organic compounds (BVOCs) that can undergo atmospheric oxidation reactions to produce secondary organic

^aSchool of Chemistry, University College Cork, Cork, T12 YN60, Ireland. E-mail: julien.Kammer@univ-amu.fr

^bEnvironmental Research Institute, University College Cork, Cork, T23 XE10, Ireland

^cSchool of Biological, Earth and Environmental Sciences, University College Cork, Cork, T23 TK30, Ireland

^dDepartment of Food Quality and Sensory Science, Teagasc Food Research Centre, Moorepark, Fermoy, Cork, P61 C996, Ireland

^eSchool of Food and Nutritional Science, University College Cork, T12 R220, Ireland

^fAix Marseille Univ., CRNS, LCE, Marseille, 13331, France

† Electronic supplementary information (ESI) available. See DOI: <https://doi.org/10.1039/d4ea00138a>



aerosols (SOA), which contribute to climate forcing.^{8,9} Therefore, it is important to determine the BVOC emission profile of a species to help understand the potential atmospheric impact of establishing large-scale plantations.

BVOCs are emitted by plants through either a biosynthetic pathway, pooled emission pathway or a combination of both of these mechanisms. In the biosynthetic pathway, BVOCs are synthesised within the chloroplasts of the plant and are emitted immediately.¹⁰ Biosynthetic pathways only operate in the presence of light, and are strongly influenced by photosynthetically active radiation (PAR),¹¹ measured as photosynthetic photon flux density (PPFD), as well as temperature.¹² In the pooled emission pathway, BVOCs are synthesised, deposited in storage pools and released later.¹² The emission of BVOCs from storage pools occurs under both dark and light conditions, does not depend on PAR, but has a strong relationship with temperature.¹³ The BVOCs are assumed to diffuse out of the storage pools, with the rate of diffusion related to the vapour pressure of the specific BVOC.¹⁴ PPFD and temperature are the main drivers for BVOC emissions, although other environmental and plant conditions also contribute, including precipitation, season, age and stress.^{15–17}

Numerous field and laboratory studies have been conducted to determine the composition of BVOC emissions, and to probe the factors (PPFD, temperature, stress *etc.*) that influence their release into the atmosphere. Although not conducted under real-world conditions, laboratory studies have the advantage of providing a controlled environment for investigating the parameters that affect BVOC emissions in a systematic manner.¹⁸ BVOC emission studies are typically conducted over a range of environmental conditions and, to facilitate comparison between studies, BVOC emission fluxes are reported at standard conditions of 30 °C and 1000 $\mu\text{mol m}^{-2} \text{s}^{-1}$. For studies conducted under different temperature and PPFD conditions a standardisation procedure is applied to convert the collected data to standard conditions.¹²

A small number of previous studies have been conducted on the BVOC emissions from Sitka spruce. The monoterpenes myrcene and β -phellandrene were found to dominate the BVOC emissions,¹ with a significant contribution also from isoprene.¹⁸ These earlier studies focussed primarily on the detection of hydrocarbons using offline GC-MS techniques, with only the most recent study using proton transfer reaction-mass spectrometry (PTR-MS)¹⁹ for online measurements. Advances in the instrumentation used for detecting ambient VOCs have led to the development of the high resolution online time-of-flight chemical ionisation mass spectrometer (ToF-CIMS),²⁰ which enables real-time detection of a wider range of emitted BVOCs, including oxygenated species.^{21,22}

Given the dominance of Sitka spruce within afforestation programmes, further work is required to identify the BVOC emissions from Sitka spruce and to assess their climatic impacts. The aims of this work were (i) to use a ToF-CIMS and thermal desorption gas chromatography mass spectrometry (TD-GC-MS) for identification of the BVOCs emitted by Sitka spruce, in a laboratory setting under different environmental

conditions, (ii) to determine the emission pathways and standardised emission fluxes for each BVOC.

2. Materials and methods

2.1 Experimental set-up

Three Sitka spruce saplings were included in this study. The saplings were grown from seed since spring 2017, at Fermoy Woodland Nursery, Co. Cork, Ireland. In January 2020, they were placed in cold storage, where they took on a state of dormancy. In July 2020, the trees were planted in individual 5 L pots containing a peat soil. Emission experiments began in November 2021, placing the sapling inside a plant growth chamber (Panasonic MLR-352). At this stage, the spruce saplings were approximately four years old, and ranged in height from 60 cm to 75 cm. The trees were watered twice a week with 350 mL of tap water each, and did not receive any fertiliser treatment. For identification purposes the saplings were named; spruce 1, spruce 2 and spruce 3 (Fig. S1†). All saplings had dark green needles, with spruce 1 having the largest amount of foliage and spruce 3 the least. Spruce 1 and spruce 3 had visible resin deposits on their trunks (Fig. S2†). A month prior to emissions sampling spruce 1 produced new shoots, the majority of which were outside the enclosure.

The overall set-up for emissions sampling is shown schematically in Fig. 1 and is based on dynamic emissions chambers (Fig. S2†) described previously.²³ Filtered outdoor air was passed over the saplings enclosed in individual Teflon enclosures and an empty enclosure (for background measurements) housed inside the plant growth chamber. The two interior side walls and door of the plant growth chamber were each equipped with five photosynthetically activating lamps (Panasonic FL40SSW/37-PRF3 Fluorescent Lamps). The lamps extended from the floor to the ceiling and provided a PPFD range from 0 $\mu\text{mol m}^{-2} \text{s}^{-1}$ (no lamps illuminated) to 250 $\mu\text{mol m}^{-2} \text{s}^{-1}$ (all lamps illuminated when empty). The temperature was adjustable between 5 °C and 40 °C. Further details of the set-up are provided in the ESI.†

Outdoor air was sampled through an open window at 32 L min⁻¹ with a pump (Becker VT4.4) and passed through a zero air scrubber (OPT 86C, Teledyne) and a home-made activated charcoal filter (Hatchwells granulated charcoal) to remove atmospheric oxidants and VOCs, as well as a HEPA filter (TSI) to remove particles. The filtered air flow rate into each enclosure was set to a fixed value between 4.5 and 7 L min⁻¹. Temperature and relative humidity measurements (dewpoint probe DMP74A, Vaisala) were taken from inside a miniature enclosure to account for any changes in conditions due to the presence of the enclosure.²⁴ The miniature enclosure was sealed around one of the lower branches of spruce 1 and was supplied with the same filtered air.

The use of a flow-through multivalve (Multiposition actuator EMTMA-CE, Vici Valco) allowed rapid and controlled sample switching between the various enclosures. The outflows from the three spruce enclosures and empty enclosure were each connected to an inlet on the multivalve. At any time, a single inlet was connected to the sample port which supplied the ToF-



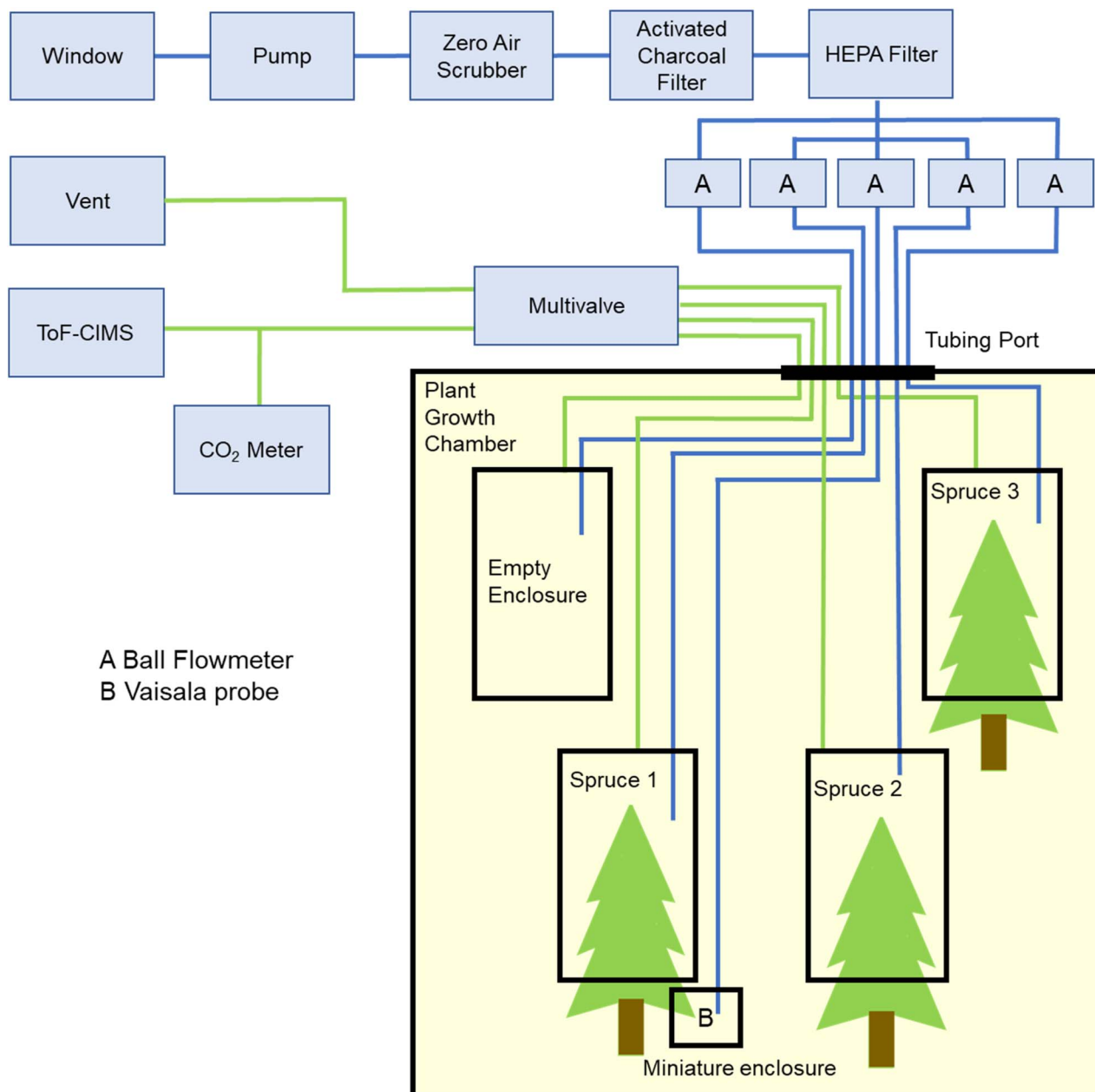


Fig. 1 Schematic of emissions sampling set-up.

CIMS and CO₂ meter, while the remaining inlets were connected to the exhaust which was externally pumped to ensure that all lines were continually flushed to prevent dead volume effects. The multivalve was programmed to connect the sample port with each inlet for 7.5 min, in the following order: empty enclosure, spruce 1, spruce 2, spruce 3. This 30 min cycle was continuously repeated. The remaining flows were vented to avoid dead volume and tubing memory effects.

2.2 Experimental procedures

Three different 24 hour plant growth cycles were used to assess the impact of temperature and PPFD on BVOC emissions from the Sitka spruce. Prior to each sampling cycle, the enclosure around the saplings were sealed and acclimation period of 2–3

days was applied to allow the saplings sufficient time to adapt to the new environment, which included the enclosure around the branch. As the emissions were sampled from only three saplings, measurements were recorded for a minimum of 7 consecutive days to maximise reproducibility for statistical purposes.

For the daily cycle the saplings were subject to conditions closely resembling those for the Irish summer, in which both temperature and PPFD increase simultaneously to a maximum and decrease. BVOCs and CO₂ were measured and used to assess variations in emissions and photosynthesis due to changes in PPFD and temperature.

The conditions for the daily cycle were a repeating 24 hours cycle comprising: 10 hours of darkness at 12 °C; 3 hours at 21



$\mu\text{mol m}^{-2} \text{s}^{-1}$ and 15 °C; 3 hours at 44 $\mu\text{mol m}^{-2} \text{s}^{-1}$ and 18 °C; 2 hours at 164 $\mu\text{mol m}^{-2} \text{s}^{-1}$ and 21 °C; 3 hours at 44 $\mu\text{mol m}^{-2} \text{s}^{-1}$ and 18 °C; and 3 hours at 21 $\mu\text{mol m}^{-2} \text{s}^{-1}$ and 15 °C (Fig. S4†). While these PPFD levels are representative of the average daily summer conditions in Ireland, values up to 1000 $\mu\text{mol m}^{-2} \text{s}^{-1}$ can be experienced on very sunny days, which may potentially change BVOC emissions profiles in these conditions.

The purpose of the temperature cycle was to determine the effect of temperature on BVOC emissions and photosynthesis. The conditions for the temperature cycle were: 4 hours of darkness at 12 °C; 3 hours of darkness at 15 °C; 3 hours of illumination at 15 °C; 3 hours of illumination at 18 °C; 2 hours of illumination at 21 °C; 3 hours of illumination at 18 °C; 3 hours of illumination at 15 °C; and 3 hours of darkness at 15 °C (Fig. S5†). During the hours of illumination, a constant PPFD of 44 $\mu\text{mol m}^{-2} \text{s}^{-1}$ was applied.¹⁴

The purpose of the light cycle was to identify changes in BVOC emissions and photosynthesis resulting from variations in PPFD only. A constant temperature of 18 °C was applied for the duration of the light cycle and the PPFD was varied according to: 10 hours of darkness; 3 hours at 21 $\mu\text{mol m}^{-2} \text{s}^{-1}$; 3 hours at 44 $\mu\text{mol m}^{-2} \text{s}^{-1}$; 2 hours at 164 $\mu\text{mol m}^{-2} \text{s}^{-1}$; 3 hours at 44 $\mu\text{mol m}^{-2} \text{s}^{-1}$; and 3 hours at 21 $\mu\text{mol m}^{-2} \text{s}^{-1}$ (Fig. S6†). After completion of the three plant growth cycles, air samples were collected onto previously conditioned sorbent tubes (Markes Tenax TA, C1-CAXX-5003) at a flow rate of 200 mL min^{-1} for 2 hours.

Four samples (one sample from each enclosure) were collected with conditions in the plant growth chamber set to 44 $\mu\text{mol m}^{-2} \text{s}^{-1}$ and 18 °C and four samples were collected with conditions in the plant growth chamber set to 164 $\mu\text{mol m}^{-2} \text{s}^{-1}$ and 24 °C. To account for any potential residue remaining on the Tenax tubes from previous use, two tubes were left unopened and deemed to be sample blanks. Sampling onto the Tenax tubes did not commence until an hour after the conditions in the plant growth chamber had been set.¹⁸ After sampling, the Tenax tubes were sealed using Swagelock brass caps and Teflon ferules, individually wrapped in aluminium foil, placed into separate zip lock bags, and stored in a refrigerator^{25,26} until TD-GC-MS analysis could be performed.

Following all measurements, the Sitka spruce saplings were cut, and all biomass contained within the enclosures was removed, and dried at 60 °C for 72 hours¹⁹ using incubators (Memmert IN110 Incubator). When drying was completed a mass balance (Explorer OHAUS, E02140) was used to determine the dry mass of the needles only, as well as the dry mass of the needles plus branches for each sapling (Table S1†).

2.3 Instrumentation

2.3.1 ToF-CIMS. A high-resolution time-of-flight chemical ionisation mass spectrometer (ToF-CIMS, Aerodyne C4Q-106) was used to monitor the BVOC emissions from the Sitka spruce saplings in real time. The general operation of the ToF-CIMS has been described elsewhere.^{20,27} The ToF-CIMS used in this work was fitted with a VUV ionisation source.²⁸ The benzene cation

(C_6H_6^+) was selected as the reagent ion for these measurements because of its ability to ionise compounds with a low oxygen content, as well as hydrocarbons such as monoterpenes, which are typical of biogenic emissions.²⁹ Benzene vapour was generated by flowing N_2 (BOC, oxygen free) at a rate of 0.25 L min^{-1} over a liquid benzene permeation tube (6-PD-1400-C45, Carl Stuart Group) placed inside $\frac{3}{4}$ " stainless steel tubing, which was maintained at 50 °C. The benzene vapour passed into the VUV source where C_6H_6^+ was formed *via* the ejection of an electron.³⁰ The voltages and pressures applied to the ToF-CIMS were controlled *via* TOFWERK TPS settings. Trichlorobenzene (Sigma Aldrich, 99%), was used as an internal mass calibrant, by allowing it to diffuse into the inlet of the instrument.

To quantify BVOCs, calibration coefficients were determined for δ -3-carene, β -myrcene, camphor (Sigma Aldrich, purity 90%, 75% and 98%, respectively) and piperitone (Santa Cruz Biotechnology, purity >94%), by injecting aliquots of BVOC into a 2.2 m^3 atmospheric simulation chamber at the Environmental Research Institute, University College Cork.³¹ The concentrations of BVOCs emitted by the Sitka spruce saplings were below the range of the linear calibration plots, and it was therefore assumed that the ToF-CIMS continued to have a linear response over the full range of concentrations measured during BVOC emissions sampling and calibrations.²⁷ The calibration coefficients for the four BVOCs were applied to the various ions detected by the ToF-CIMS.

Data collected by the ToF-CIMS were analysed with Tofware 3.2.0, operated through IGOR Pro 7.08. Firstly, 1 Hz data were averaged to a 10 s time resolution. Following this, the recommended Tofware calibration and correction steps were performed. Chemical formulae containing the elements C, H, O, N and Cl were then assigned to peaks within the calibrated mass range. If an appropriate formula could not be determined, the peak was left unassigned, and excluded from further analysis. After the peak assignments were completed, data points recorded during periods of interference (disconnection of the CO_2 meter and contamination of outdoor air by a species producing $\text{C}_{10}\text{H}_{15}^+$ in the ToF-CIMS) were removed.

2.3.2 TD-GC-MS. The sorbent tubes were placed on the tray of an autosampler (unity 2 Autosampler, Markes International Ltd.) and subsequently introduced to the unity 2 thermal desorption unit (Markes International Ltd.), which was connected by a heated transfer line to the column of a gas chromatograph mass spectrometer (Agilent Technologies 7890A GC and Agilent 5977B MSD). The first step of the desorption involved dry purging the tubes for 2 min using a 1 : 20 split with N_2 at 50 psi, before undergoing a 5 min thermal desorption at 150 °C, followed by a secondary desorption at 280 °C for 5 min. BVOCs were collected onto a materials emissions trap held at 30 °C with a gas flow of 50 mL min^{-1} . A 2 min fire purge was then applied to the trap with a 1 : 50 split, the BVOCs were desorbed from the trap using a temperature ramp of 24 °C min^{-1} with a 1 : 10 split for 5 min. The transfer line was heated to 160 °C, the GC injector was set at 250 °C and operated in splitless mode. Chromatographic separation was achieved using a 60 m capillary column (Agilent Technologies Ltd, DB 624UI 60 m × 0.3 mm × 1.8 μm , 0.32 mm inner diameter) and helium as the carrier gas at a constant



pressure of 23 psig. The column temperature was initially held at 40 °C for 5 min, and then increased at a rate of 5 °C min⁻¹ to 230 °C, held for 35 min with a total run time of 78 min. The mass spectra were generated by the quadrupole MS detector with ionisation voltage of 70 eV, 3.32 scans s⁻¹. The ion source temperature was 230 °C and the interface temperature was set at 280 °C.

The chromatograms generated from each tube were analysed with MassHunter Qualitative Analysis Navigator (B.08.00, 2016). BVOC identification was verified using retention indices and fragmentation patterns compared to an in-house spectral library and the NIST 2014 mass spectral library with the assistance of deconvoluting software AMDIS (v2.72, June 2014). Linear retention indices were determined using established methods (Van Den Dool and Dec. Kratz, 1963). In addition, BVOC isomers in the Sitka spruce emissions were separated by TD-GC-MS and identified with the use of standards. The presence of isoprene, α -pinene, β -pinene, myrcene, camphene, camphor (Sigma Aldrich, purities 99%, 98%, 99%, 75%, >96% and 98% respectively) and piperitone (Santa Cruz Biotechnology, purity 94%) were verified in the Sitka spruce emissions.^{32,33} The BVOCs were dissolved in methanol and subsequently in distilled water to obtain a mixing ratio of 10 ppm. A 10 μ L volume of each standard was transferred onto Tenax tubes and analysed on the TD-GC-MS system under the same conditions as the Sitka spruce samples. An auto-tune of the GC-MS was carried out prior to the analysis to ensure optimal performance. A set of external standards was run at the start and end of the sample set and abundances were compared to known amounts to ensure that both separation and MS detection were performing within specification.

2.3.3 Ancillary measurements. A CO₂ meter (K30 ELG 10,000 ppm CO₂ data logging sensor) was used to monitor CO₂ uptake and emission by the saplings, to determine photosynthetic activity and respiration. The CO₂ meter was operated with GasLab software and recorded a measurement every 10 s. The sensor background was controlled using pure N₂ (BOC, oxygen free) and a calibration up to 911 ppm was performed by adding pure CO₂ (BOC, 99%) to an atmospheric simulation chamber.

A light meter (LI-250, LI-COR light meter) was used to measure PPFD in the centre of the plant growth chamber with all three Sitka spruce saplings and enclosures present (Table S4†). The measurements were taken before and after the emissions sampling cycles. The plant growth chamber door remained closed during PPFD measurements. The average PPFD values recorded at the three light settings were 21 μ mol m⁻² s⁻¹, 44 μ mol m⁻² s⁻¹ and 164 μ mol m⁻² s⁻¹.

A chlorophyll fluorescence meter (Hansatech FMS2) was used to determine maximum photosystem II efficiency (F_v/F_m) of the Sitka spruce. Chlorophyll fluorescence measurements were recorded twice a day, three days per sampling cycle. One measurement was taken 30 min prior to illumination and a further measurement was taken 90 min into the maximum PPFD and temperature setting. Three branches on each sapling were selected for measurements. Clips were placed over the needles for dark adaptation for 30 min before each measurement.

2.4 Emission calculation and modelling

The last 2 min of the 7.5 min sampling period for each of the four enclosures was used to generate 30 min average values for BVOC concentrations and CO₂ mixing ratios. These values were subsequently analysed using R Studio 4.0.2 to determine BVOC and CO₂ fluxes for each measurement cycle.

The CO₂ fluxes for each spruce sapling were calculated using eqn (1):

$$\text{Flux}_{\text{CO}_2} = \frac{(\text{spruce}_{\text{CO}_2} - \text{empty}_{\text{CO}_2}) \times \text{flow} \times \text{factor}_{\text{CO}_2}}{N_A \times \text{biomass}}, \quad (1)$$

where Flux_{CO₂} is the CO₂ flux in nmol s⁻¹ g⁻¹; spruce_{CO₂} is the CO₂ mixing ratio in ppm in the spruce enclosure; empty_{CO₂} is the CO₂ mixing ratio in ppm in the empty enclosure; flow is the flow through the spruce enclosure in m³ h⁻¹; N_A is Avogadro's number in mol⁻¹; biomass is the mass of the needles in g_{dw}; and factor_{CO₂} is a constant in h ppm⁻¹ m⁻³ s⁻¹, which accounts for unit conversions.

A Welch *t*-test (modified version of the Student's *t*-test) was performed on the data from the daily cycle to differentiate ions due to the BVOCs from those in the background spectra. Only ions with a *p*-value of less than 0.05 when compared with three times the ion signal from the empty enclosure, measured at a PPFD greater than 40 μ mol m⁻² s⁻¹, were attributed as statistically significant emissions. Only the ions identified in the daily cycle were analysed for the temperature cycle and light cycle. No ion signals from spruce 3 were above the statistical threshold, and therefore spruce 3 was removed from all further analysis.

The BVOC fluxes for each spruce sapling were calculated using eqn (2):

$$\text{Flux}_{\text{BVOC}} =$$

$$\frac{(\text{spruce}_{\text{BVOC}} - \text{empty}_{\text{BVOC}}) \times \text{flow} \times \text{MW}_{\text{BVOC}} \times \text{factor}}{N_A \times \text{biomass}} \quad (2)$$

where Flux_{BVOC} is the emission flux of a specific BVOC in $\mu\text{g g}_{\text{dw}}^{-1} \text{ h}^{-1}$; spruce_{BVOC} is the concentration of the BVOC from the spruce enclosure in ions s⁻¹; empty_{BVOC} is the concentration of the BVOC from the empty enclosure in ions s⁻¹; flow is the flow through the spruce enclosure in m³ h⁻¹; MW_{BVOC} is the molecular weight of the BVOC in g mol⁻¹; biomass is the mass of the dried needles and branches in g_{dw}; and factor is a constant to account for unit conversions in ions⁻¹ s⁻¹ m⁻³.¹⁹

Sitka spruce BVOC emissions have previously been reported to originate from pooled emission pathways (monoterpenes) and biosynthetic pathways (isoprene).^{18,19} For BVOCs originating from biosynthetic sources, the emission flux can be standardised to a PPFD of 1000 μ mol m⁻² s⁻¹, and a temperature of 30 °C according to the following equations developed by Guenther *et al.* (1993)¹² and adapted by Schuh *et al.* (1997):¹⁴

$$E_{\text{isoprene}} = E_{\text{isoprene}}^{\text{standard}} \times C_L \times C_T \quad (3)$$

where E_{isoprene} is the isoprene emission flux at the measured temperature and PPFD in $\mu\text{g g}_{\text{dw}}^{-1} \text{ h}^{-1}$; $E_{\text{isoprene}}^{\text{standard}}$ is the isoprene



emission flux in $\mu\text{g g}_{\text{dw}}^{-1} \text{ h}^{-1}$ at standard conditions of 30 °C and 1000 $\mu\text{mol m}^{-2} \text{ s}^{-1}$; C_L and C_T are factors to account for the PPFD and temperature dependence of the emissions respectively. C_L is described by eqn (4):

$$C_L = \frac{\alpha \times c_{L1} \times L}{\sqrt{1 + (\alpha^2 \times L^2)}}, \quad (4)$$

where α and c_{L1} are empirical constants with values 0.0027 and 1.066 respectively; and L is the PPFD in $\mu\text{mol m}^{-2} \text{ s}^{-1}$. The temperature dependence of biosynthetic emissions is described by eqn (5):

$$C_T = \frac{\exp\left(\frac{c_{T2} \times (T - T_s)}{R \times T \times T_s}\right)}{1 + \exp\left(\frac{c_{T3} \times (T - T_M)}{R \times T \times T_s}\right)}, \quad (5)$$

where c_{T2} is an empirical constant of value 95 000 J mol^{-1} ; T is the measured temperature in K; T_s is standard temperature, 303 K; R is the universal gas constant, 8.314 $\text{J K}^{-1} \text{ mol}^{-1}$; c_{T3} is an empirical constant of value 230 000 J mol^{-1} ; and T_M is the temperature of maximum enzyme activity in K (here taken as 313 K). This equation has been used in multiple studies to standardise isoprene emissions.^{24,34}

The temperature dependent term (C_T) of the biosynthesis equation (eqn (3)) was simplified with the removal of the denominator, as described previously by Schuh *et al.* (1997).¹⁴ It relies on T_M , the temperature of maximum enzyme activity, which was unknown for the Sitka spruce used in this study, but is expected to be close to 40 °C. Due to the difference between T_M and the temperatures employed in this study, the denominator can be approximated to one. Unique coefficients were calculated for each BVOC from spruce 1 and spruce 2, and were used to model spruce 1 and spruce 2 daily cycle data.

The emission of monoterpenes is reported to be mostly temperature dependent,¹⁸ although there is some evidence for a combination of biosynthetic and pooled emission pathways. The temperature dependant algorithm is described thus:

$$M = M_s \times \exp(\beta \times (T - T_s)), \quad (6)$$

where M is the measured monoterpene emission flux in $\mu\text{g g}_{\text{dw}}^{-1} \text{ h}^{-1}$; M_s is the monoterpene emission flux in $\mu\text{g g}_{\text{dw}}^{-1} \text{ h}^{-1}$ at standard temperature, β is an empirical coefficient of value 0.09 K^{-1} ; T is the measured temperature in K; and T_s is standard temperature, 303 K.

Studies by Schuh *et al.* (1997)¹⁴ on sunflower and beech found BVOC emissions to originate from a combined biosynthetic and pooled emission pathway. A combined equation was developed under the assumption that both emission pathways are completely independent, and the total emission flux is the sum of the emission flux from each pathway, described by eqn (7):

$$E_{\text{combined}} = E_{\text{pooled}} + E_{\text{biosynthesis}}, \quad (7)$$

where E_{combined} is the total emission flux in $\mu\text{g g}_{\text{dw}}^{-1} \text{ h}^{-1}$, E_{pooled} is the temperature only dependent emission flux from storage

pools in $\mu\text{g g}_{\text{dw}}^{-1} \text{ h}^{-1}$, obtained using the monoterpene emission M from eqn (6) and $E_{\text{biosynthesis}}$ is the biosynthetic emission flux, obtained using the isoprene emission E_{isoprene} from eqn (3).¹² Unique coefficients (α , c_{L1} , c_{T2} , c_{T3} and β) were derived for each BVOC emitted by spruce 1 and 2 using the measurement data from the temperature and light cycles.

All BVOC emissions were subject to three standardisation procedures; pooled, biosynthetic and combined standardisation. For each BVOC emitted from spruce 1 and spruce 2, the method that best reproduced the emission profile (based on time series) for the daily cycle was selected and used to determine the standardised emission flux.

3. Results and discussion

3.1 CO₂ fluxes

The CO₂ flux was first used to analyse whether the saplings were photosynthesising and respiring over the course of the experiments (daily cycle, temperature cycle and light cycle). The results for the daily cycle are shown in Fig. 2. For spruce 1, the CO₂ flux followed the expected trend and was highest in the dark, when photosynthesis and CO₂ uptake are not expected to occur, and mitochondrial respiration takes place. A negative CO₂ flux was observed upon illumination, which became larger as the PPFD increased. This is an indication of photosynthetic activity and plant growth.³⁵ For spruce 1 the flux in the dark varied between 0 $\text{nmol s}^{-1} \text{ g}^{-1}$ and 5 $\text{nmol s}^{-1} \text{ g}^{-1}$, similar to that previously observed for oak in the dark.³⁶ At the highest PPFD (164 $\mu\text{mol m}^{-2} \text{ s}^{-1}$) and temperature (21 °C) the CO₂ flux was approximately 15 $\text{nmol s}^{-1} \text{ g}^{-1}$, which is comparable to the value of 20 $\text{nmol s}^{-1} \text{ g}^{-1}$ measured for Norway spruce³⁷ at 23 °C and 200 $\mu\text{mol m}^{-2} \text{ s}^{-1}$. For Sitka spruce in the field CO₂ fluxes were close to 80 $\text{nmol s}^{-1} \text{ g}^{-1}$ at a minimum PPFD of 700 $\mu\text{mol m}^{-2} \text{ s}^{-1}$.³⁸

The CO₂ flux for spruce 2 was more scattered with spikes occurring regularly throughout the daily cycle. The trend was similar to that observed for spruce 1, although the magnitude of the CO₂ flux was much lower (*ca.* 3 times). However, while the photosynthetic CO₂ flux was reduced, there was no indication of chronic photoinhibition from the F_v/F_m measurements (Table S3†), which would have indicated that lower rates of photosynthetic CO₂ flux could have been caused by stomatal closure.

For spruce 3, the data were highly scattered, and there was no correlation between illumination and CO₂ flux. This suggests that spruce 3 may not have been undergoing photosynthesis effectively and was dormant during experiments.

During the temperature cycle, the CO₂ fluxes only changed slightly as the temperature was increased under constant illumination conditions (Fig. S7†). However, the effect of light was much more pronounced for both spruce 1 and spruce 2, as illumination caused a significant decrease in CO₂ due to uptake for photosynthesis.

The pattern of the CO₂ flux during the light cycle (Fig. S8†) was the same as that observed during the daily cycle, with a clear change in response to PPFD variations for both spruce 1 and spruce 2. The magnitude of the CO₂ flux during the light cycle was larger than for the daily cycle. This is somewhat



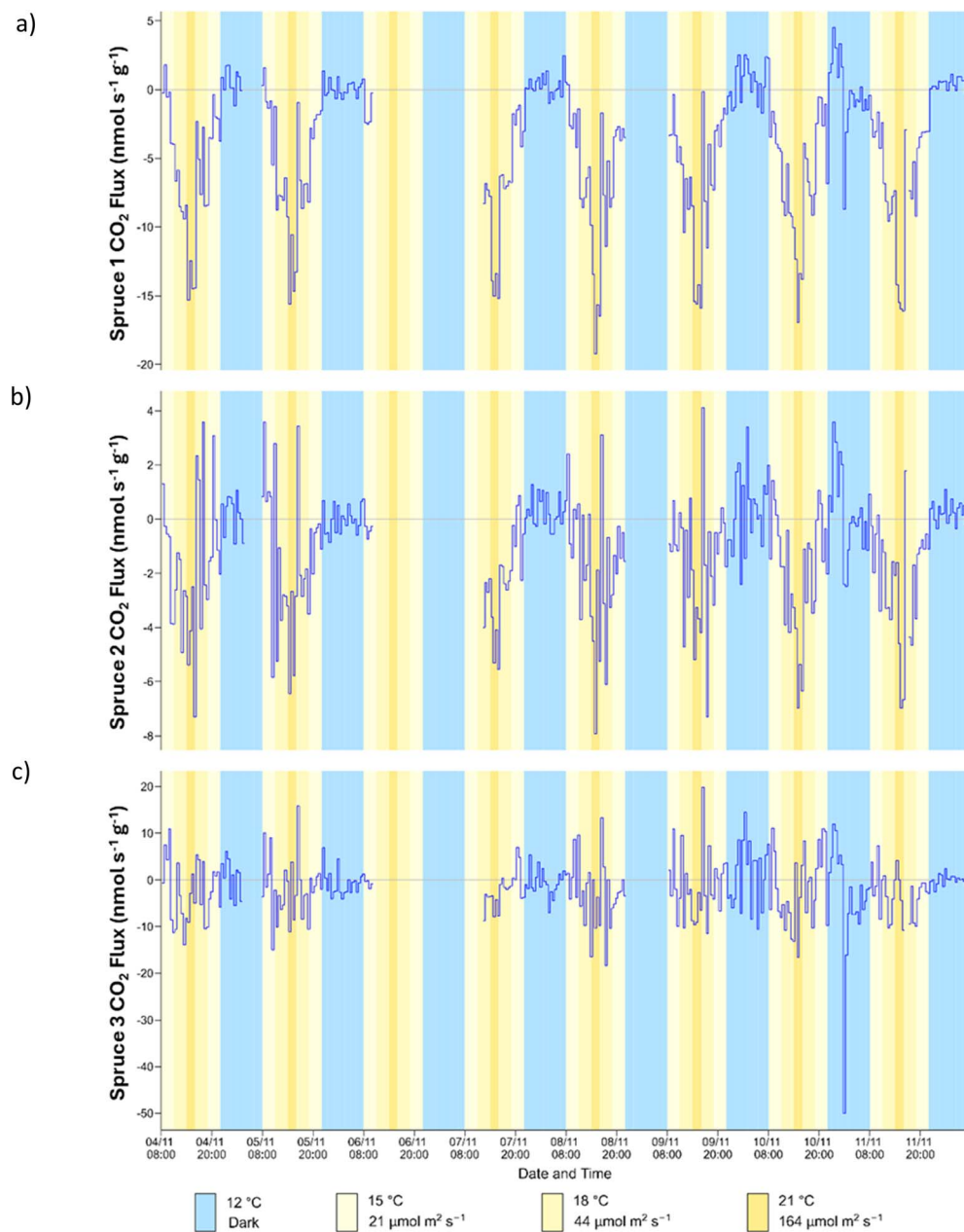


Fig. 2 Time series of CO_2 flux for (a) spruce 1 (b) spruce 2 and (c) spruce 3 during the daily cycle.

surprising as the PPF was the same for both cycles, therefore the fluxes would be expected to be similar. It may be due to the growth of the saplings as the light cycle has been performed at last, after the daily cycle and temperature cycle.

3.2 Identification of emitted BVOCs

In total 74 BVOCs were detected in the emissions from spruce 1 and spruce 2 using a combination of ToF-CIMS and TD-GC-MS. This contrasts with previous studies, which identified fewer than 10 BVOCs from Sitka spruce, including isoprene, monoterpenes and sesquiterpenes.^{1,18,19} Spruce 1 emissions contained 49 different BVOCs, while 58 species were detected in the emissions from spruce 2. As indicated above, the ToF-CIMS ion signals for spruce 3 emissions were weak and below the

statistical threshold for detection. This is consistent with the CO_2 measurements which showed that this sapling was dormant and showed no photosynthetic activity during the experiments.

A summary of the molecular formulae and compounds detected by ToF-CIMS and TD-GC-MS respectively is given in Fig. 3 and Table S2.† While there were some differences between spruce 1 and spruce 2, the pattern of BVOC emissions was very similar, spanning C_3 to C_{20} , with the majority of species in the range C_5 – C_{10} . Furthermore, 21 of the compounds identified by TD-GC-MS and numerous other molecular formulae were common to both saplings. Interestingly, the majority (70%) of the BVOCs detected were oxygenated species, containing up to 5 O atoms.

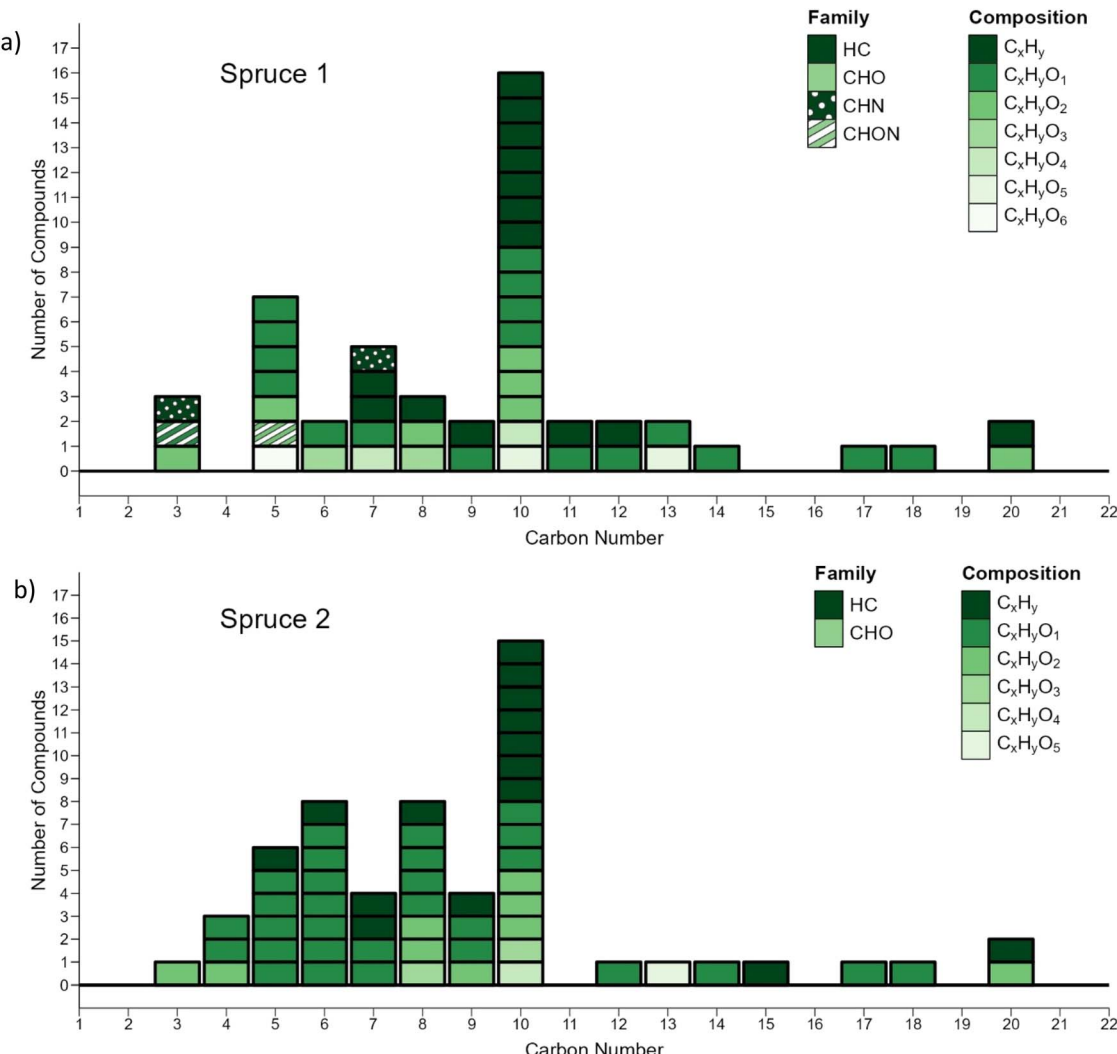


Fig. 3 Distribution of the molecular formulae for BVOCs detected by ToF-CIMS and TD-GC-MS emitted by (a) spruce 1 and (b) spruce 2.

This observation is somewhat different from reports in the literature, which typically identify isoprene,^{39,40} monoterpenes^{18,19} and sesquiterpenes⁴¹ as the dominant biogenic emissions from plants.

The contribution from oxygenated BVOCs is usually quite low in BVOC emission studies, and reporting is typically restricted to specific groups: small compounds such as acetone⁴² and methanol;⁴³ green leaf volatiles (GLVs);⁴⁴ and the $C_{10}H_{18}O$ isomers, including linalool⁴⁵ and eucalyptol.⁴⁶ Few studies have reported oxygenated BVOCs that fall outside these groups.^{47,48} The high proportion of oxygenated BVOCs detected in this study is most likely due to the measurement capabilities of the instrumentation used. The use of benzene cations ($C_6H_6^+$) in ToF-CIMS is well suited to the detection of hydrocarbons and certain oxygenated compounds.⁴⁹ In contrast, GC-MS and PTR-MS, which are traditionally used in the analysis of BVOCs, tend to focus on the detection of hydrocarbons and small oxygenated compounds.^{18,50}

Moreover, the ToF-CIMS is generally better than PTR-MS at detecting oxygenated species containing two or more O atoms.²² In this work, O_2 – O_5 species represent 13% and 9% of all

emissions from spruce 1 and spruce 2 respectively. The detection of species with up to five O atoms is particularly interesting because the presence of such highly oxygenated compounds is generally considered to be due to secondary formation in the atmosphere, as opposed to primary emissions, which is the case here.

An oxygenated monoterpene, piperitone ($C_{10}H_{16}O$) was the main BVOC emitted from spruce 1 and the second highest emission from spruce 2, representing 28% and 27% of the BVOC emissions respectively, based on median emissions during the daily cycle (Fig. S9†). Piperitone has been identified as a BVOC emission in previous studies, but never as the main emitted BVOC. Piperitone was identified as a minor emission from damaged Sitka spruce branches, with the sum of the concentration of the isomers piperitone and camphor found to be over an order of magnitude lower than the sum of monoterpene concentration.³³ The elevated piperitone concentration in this work may be related to differences in environmental conditions between this work and other studies, or due to different chemotypes, as previously reported for Scots pine.⁵¹



Piperitone has also been detected as a BVOC emitted by Norway spruce⁵² and Ponderosa pine.⁵³

Several studies on the needle oil^{54–56} and cortical resin⁵⁵ of Sitka spruce found it to be composed mainly of myrcene ($C_{10}H_{16}$), and two $C_{10}H_{16}O$ isomers, piperitone and camphor. In all studies, the proportion of piperitone in the leaf oil and cortical resin was always greater than camphor. The detection of camphor in the BVOC emissions of Sitka spruce,^{32,33} is more common than for piperitone, implying that in the emissions camphor is the dominant isomer. However, in this work, piperitone was much more abundant than camphor and the ratio of piperitone to camphor was similar to that reported in the literature for resin. Importantly, resin deposits were visible on the trunk of spruce 1 and may also have been present on spruce 2 (Fig. S2†). The high piperitone to camphor ratio observed in this study therefore indicates that evaporation from the resin deposits may have contributed to the BVOC emissions detected from the Sitka spruce saplings.

The sum of monoterpenes ($C_{10}H_{16}$) was the highest emission from spruce 2 (28% of all emissions) and the third highest emission from spruce 1 (13%, Fig. S9†). Five monoterpenes were detected, myrcene, β -phellandrene, α -pinene, δ -limonene and camphene, all of which have previously been reported as Sitka spruce emissions. The same isomers were detected from both saplings, although the relative contributions were slightly different. In agreement with previous studies,^{1,18,40} myrcene was the dominant monoterpene emitted from both saplings (inferred from chromatogram peak areas, available in the associated dataset), followed by β -phellandrene,^{1,18} which has also been previously detected in the emissions of other spruce species.^{1,32} The α -pinene^{32,40,57} and δ -limonene also made a substantial contribution to the monoterpene emissions from spruce 2; in contrast to the monoterpene mixture emitted from spruce 1 which had higher amounts of α -pinene than δ -limonene. The contribution from camphene^{32,40,57} was low for both saplings. Some studies have reported β -pinene^{18,32,33} as a major emission from Sitka spruce, but it was not identified by TD-GC-MS in this work.

The second highest emission from spruce 1 was isoprene (C_5H_8), but for spruce 2 it was not present in the ToF-CIMS analysis and was only detected at trace levels in the TD-GC-MS analysis (Table S2, Fig. S9† and associated dataset).

A similar phenomenon has been observed for Scots pine, in which δ -carene was a dominant emission from one chemotype, and not emitted from the other.⁵¹

This further supports the idea that saplings of the same species can have different emission profiles. Isoprene has been detected in the emissions of various spruce species, including Sitka spruce,^{18,19,32} Norway spruce,^{37,58} and several others.^{13,59} Isoprene has been reported as a minor emission for other coniferous species including Scots pine,³⁴ although is it more commonly found in the emissions from deciduous species such as Holm oak⁶⁰ and willow.⁶¹

The third highest emission from spruce 2, C_6H_8O , was not detected in the emissions of spruce 1 and a structure was not confirmed by TD-GC-MS (Fig. S7†). In total, six of the detected BVOCs that were unique to spruce 2 are C_6 compounds, some of

which are known to be GLVs,⁴⁴ such as *E*-2-hexenal.⁶² GLVs are emitted from plants in response to stress, such as wounding,^{35,63} infestation⁶² or drought.⁶⁴ The C_6H_8O compound may also be a GLV, emitted by Sitka spruce in response to stress. In addition, a sesquiterpene, *E*- β -farnesene, was detected in the spruce 2 emissions. Elevated levels of sesquiterpenes have been observed in the emissions of ozone stressed plants.^{65,66} In other studies the emission of farnesenes from Norway spruce⁵² and Scots pine⁵¹ were found to be elevated due to infestation. Although all saplings in this work were exposed to the same conditions, the presence of C_6 GLVs and *E*- β -farnesene indicate that spruce 2 may have been stressed. Interestingly, spruce 2 had no visible signs of stress, *e.g.*, herbivores or disease, and the F_v/F_m values were similar to those for spruce 1 (Tables S3–S5†) indicating that stress-induced photoinhibition was not a major factor. In addition, spruce 2 CO_2 fluxes showed that the sapling was still photosynthesizing throughout the experiments. This combination of observations implies that spruce 2 BVOC synthesis pathways might have been slightly affected by an unknown factor, without causing chronic photoinhibition.

3.3 Influence of environmental parameters

The time series obtained during the daily cycle show that all BVOC emissions responded to the simultaneous changes in temperature and PPF, as expected. The BVOC emission fluxes were at their highest when both temperature and PPF peaked and were at their lowest during the hours of darkness at the lowest temperature. Fig. 4 shows the time series profile for the emission of piperitone, isoprene and monoterpenes from spruce 1 during the daily cycle.

The emission of piperitone from spruce 1 was lowest during the hours of darkness at 12 °C. Upon illumination of the plant growth chamber to 21 $\mu\text{mol m}^{-2} \text{s}^{-1}$ and temperature increase to 15 °C, the emission of piperitone increased immediately and reached a new steady state (Fig. 4). The emission increased with a further 3 °C rise in temperature and doubling of the PPF. A sharp increase in emission was observed following the transition to 21 °C and 164 $\mu\text{mol m}^{-2} \text{s}^{-1}$. The emission flux took longer to stabilise at these settings, likely due to the significant increase in PPF. As the conditions were cycled back to darkness, the BVOC emission fluxes decreased accordingly. For a given temperature and PPF the emission flux attained a certain value, irrespective of short-term history (*i.e.*, preceding conditions).

The time series for most other BVOCs emitted from spruce 1 followed a similar pattern to those shown in Fig. 4. The magnitude of the change in flux at the different steps depended on the BVOC, with some species showing a pronounced increase in emission upon illumination, and others having a more muted response. The relationships between BVOC emission fluxes and light and temperature have been reported for many species of trees and plants.^{18,67} In the field, BVOC emissions have been reported to be at their lowest at night, and highest during the day when temperature and PPF reach a maximum,⁵⁸ as observed in this work.



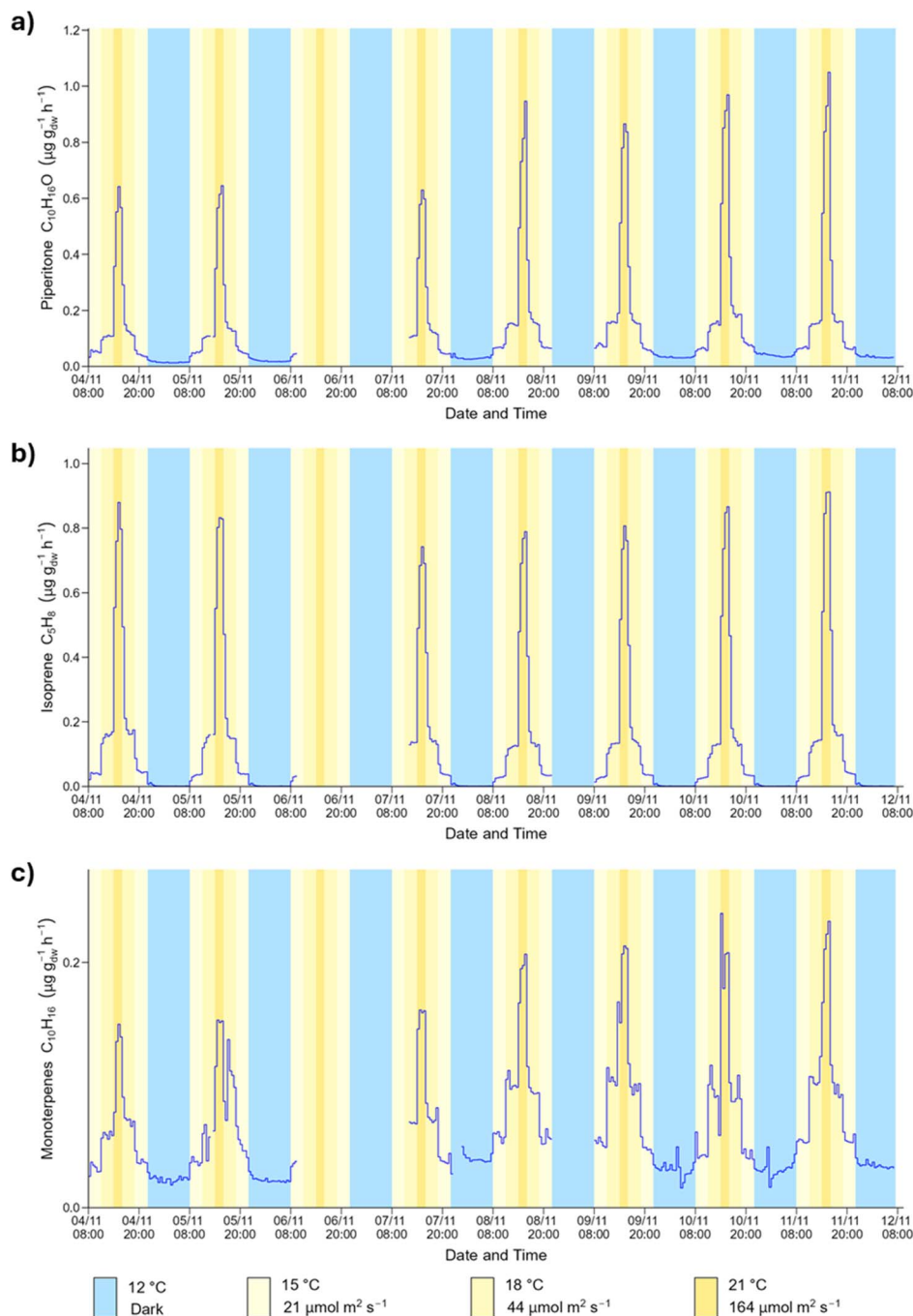


Fig. 4 Time series of (a) piperitone (b) isoprene and (c) monoterpenes emission fluxes from spruce 1 during the daily cycle. The blue colour represents nighttime, while the various shades of yellow represent daytime periods with different light and temperature conditions.

The time series profile shown in Fig. 4 is representative of the emission profile of the 34 BVOCs detected by ToF-CIMS in the spruce 1 emissions. For some BVOCs, a spike in emission was observed immediately after the lamps in the plant growth chamber were turned off. This phenomenon was observed for isoprene, $C_5H_8O_2$, $C_{10}H_{10}$, $C_{12}H_{16}$ and $C_{12}H_{20}O$ but was particularly prominent for $C_{11}H_{14}O$ (Fig. 5). An analogous event was previously observed for isoprene emitted from Sitka spruce, which was also accompanied by a spike in acetaldehyde.¹⁹ Although acetaldehyde was not measured in this work (due to

the ToF-CIMS low m/z cut off), the lifetime (a few minutes) of the spike in emissions is similar. Post-illumination acetaldehyde bursts have been observed for other tree species including oak and poplar⁶⁸ and are proposed to originate from a biological process in which acetaldehyde is produced from an excess of pyruvate *via* a pyruvate overflow mechanism.¹⁹

The BVOC emission patterns from spruce 2 during the daily cycle, were similar to those observed for spruce 1, but not as well defined. As shown in Fig. S10,† the emissions of piperitone and the sum of monoterpenes were lowest in the dark and peaked

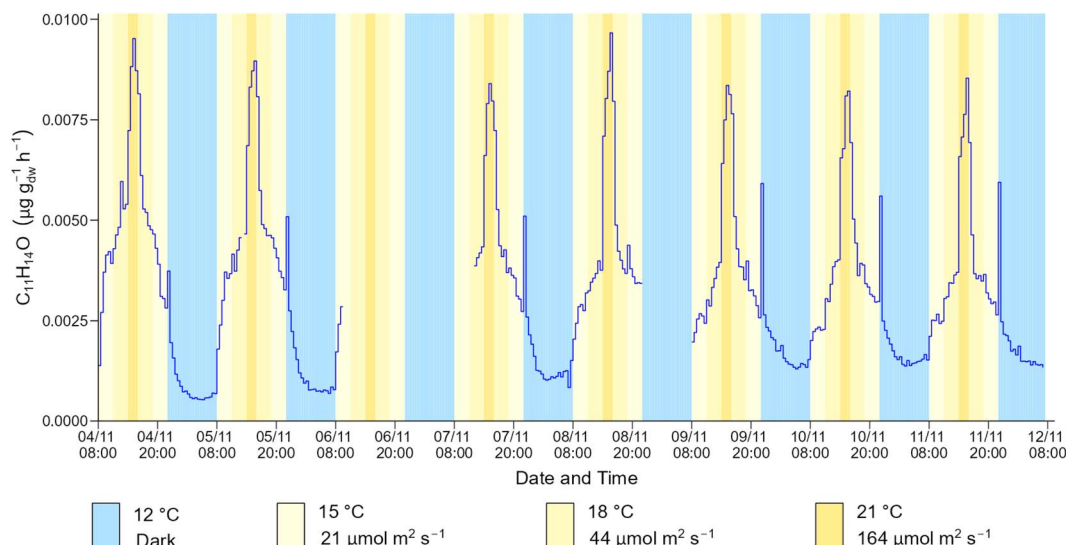


Fig. 5 Time series of the $C_{11}H_{14}O$ emission flux from spruce 1 during the daily cycle.

during the highest temperature and light conditions. However, for the intermediate conditions there was little difference observed in the emission fluxes. In addition, the fluxes did not always stabilise after a change in conditions, which might be related to the lower photosynthetic activity observed for spruce 2. The emission pattern across the week-long sampling period was also less reproducible than spruce 1, even though the order of magnitude remained in the same range.

The CO_2 and BVOC measurements obtained for spruce 1 during the daily cycle have been used to provide a first rough estimate for the contribution of BVOCs to net ecosystem carbon balance, which is an assessment of all inward and outward fluxes of carbon associated with an ecosystem.⁶⁹ The results indicate that carbon loss due to BVOC emissions accounts for approximately 0.2% of carbon taken in as CO_2 (Table S6†). Although there is considerable uncertainty associated with this estimate, which is based on data from one sapling and does not account for annual changes in environmental conditions or tree ages, the value is in reasonable agreement with previous studies conducted on other species.^{69–72}

3.4 Identification of BVOC emission pathways

The data generated during the different light and temperature cycles has been used to determine the contribution of emission pathways (pooled, biosynthetic or combined) for the BVOCs. The analysis is based on the results from spruce 1 because it was the sapling with the most reproducible emissions and the highest photosynthetic activity.

3.4.1 Pooled emissions. For the temperature cycle, the PPFD was held constant during the hours of illumination and the temperature was varied. The purpose of this cycle was to assess the contribution that temperature made to the emission flux, elucidating the importance of pooled BVOC emissions.

The average diurnal emission profile for piperitone and sum of monoterpenes from spruce 1 during the temperature cycle are shown in Fig. 6. Increasing the temperature from 12 °C to

15 °C in the dark caused a slight increase in the emission flux, while raising the temperature from 15 °C to 21 °C under constant illumination conditions resulted in an even larger increase in emission flux. Similar profiles were observed for the majority of spruce 1 BVOCs detected by ToF-CIMS, with the increased emissions at higher temperature confirming the importance of the pooled emission pathway. A temperature dependence has previously been observed for the emission of isoprene and monoterpenes from Sitka spruce,^{18,19} while a correlation between oxygenated BVOCs and temperature has also been reported for sunflower¹⁴ and aspen.⁷³ However, isoprene, along with $C_5H_8O_2$, $C_{10}H_{10}$, $C_{12}H_{16}$, $C_{12}H_{21}O$ and a few other species emitted by spruce 1, did not show any significant variation with temperature, indicating that they are unlikely to originate from storage pools.

Fig. 6 also shows an increase in emissions when the lamps were turned on while the temperature was maintained at 15 °C, indicating that light (*i.e.*, the biosynthetic pathway) also plays a role in the emission of piperitone and monoterpenes from spruce 1. For the majority of the other BVOCs, the change in emission flux with temperature was similar to that for piperitone, with the flux stabilising at each temperature setting. However, a few BVOCs, such as isoprene, experienced a continual increase in emission flux upon illumination while the temperature was maintained at 15 °C (Fig. S11†). This suggests that the emission of these BVOCs is closely linked to the biosynthetic pathway and the observed increase in emission is due to continued biosynthesis until it reaches optimum efficiency. The emission of isoprene is assumed to occur immediately following biosynthesis.¹³

3.4.2 Biosynthetic emissions. During the light cycle the temperature was maintained at 18 °C, and the PPFD was varied. The purpose of the light cycle was to determine the impact of PPFD on the Sitka spruce emissions, and to evaluate the importance of the biosynthetic BVOC emission pathway.



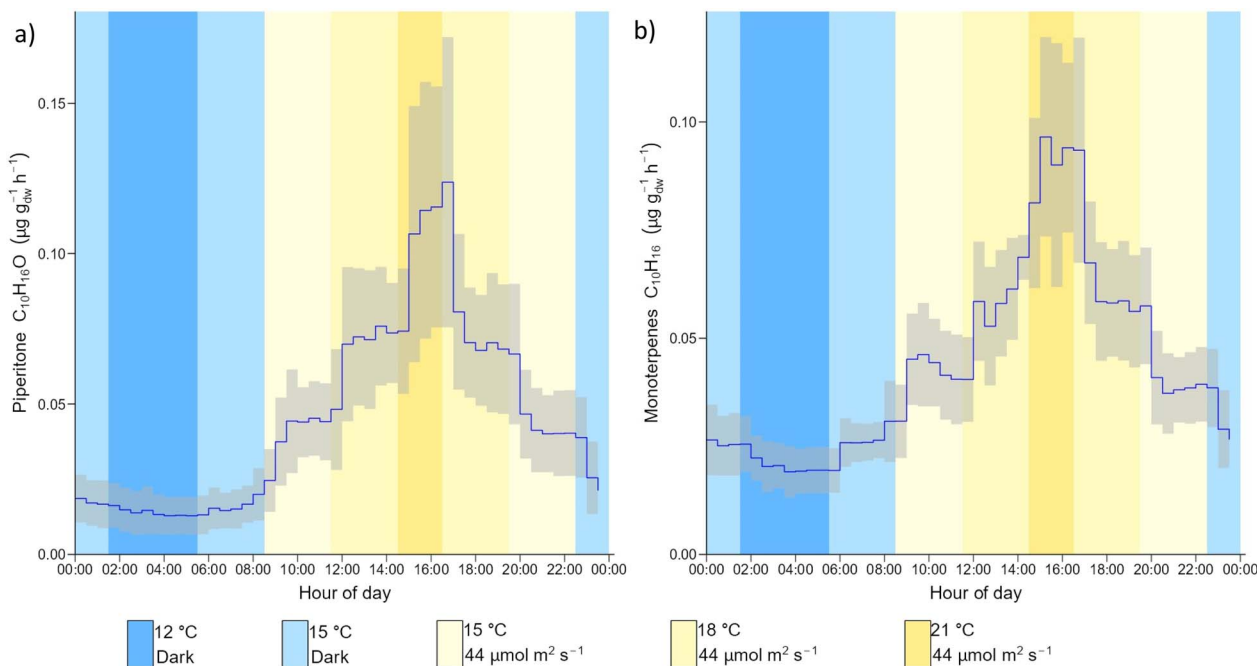


Fig. 6 Average diurnal profiles for the emission fluxes of (a) piperitone and (b) the sum of monoterpenes from spruce 1 during the temperature cycle. Blue line – measured average, grey shading – standard deviation. The diurnal plots were performed on 7 consecutive days.

Fig. 7 shows the average diurnal emission profile of piperitone emitted from spruce 1 during the light cycle. All BVOC emission fluxes from spruce 1 increased with PPFD during the light cycle. The variation in emission flux depended on the BVOC, with piperitone showing a marked change in emission flux at each PPFD setting, while other emissions, such as $C_{10}H_{12}O_2$, only showed a significant increase in emission flux at $164 \mu\text{mol m}^{-2} \text{s}^{-1}$. The emission of isoprene from Sitka spruce has previously been shown to be PPFD dependent, with the emissions of monoterpenes from Sitka spruce reported to be independent of PPFD.^{19,32} This contrasts with the results obtained here, where the

sum of monoterpene emissions from spruce 1 showed a clear response to PPFD changes. Monoterpene emissions are traditionally assumed to be temperature dependent only,¹¹ although monoterpene emissions from Norway spruce⁷⁴ and oak³⁶ have been found to also have a light dependance.

3.5 BVOC emission standardisation

3.5.1 Standardisation procedures

3.5.1.1 *Pooled emission model.* Assuming the BVOCs were emitted from pooled sources, eqn (6) was first used to model the measurement data for the daily cycle of spruce 1 and spruce 2

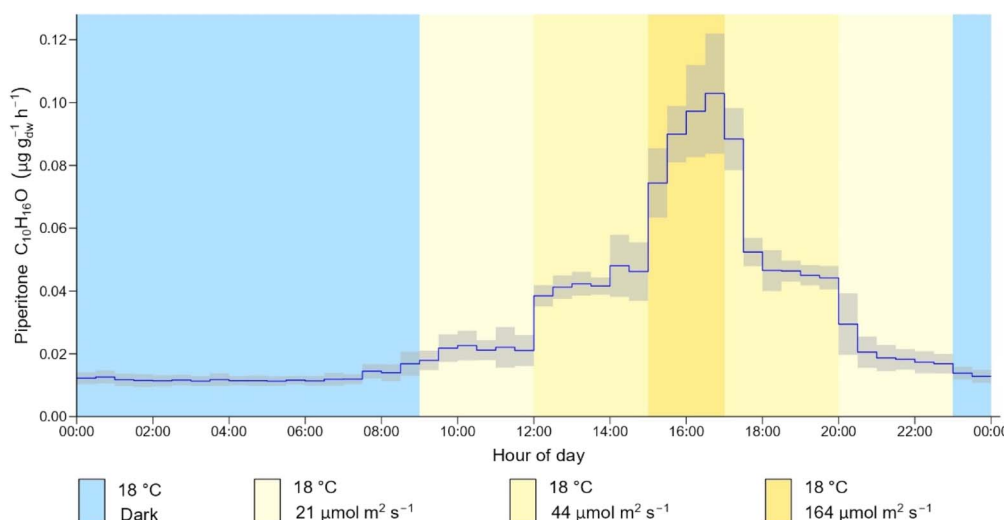


Fig. 7 Average diurnal cycle of piperitone flux from spruce 1 during the light cycle. Blue line – measured data, grey shading – standard deviation. The diurnal plots were performed on 7 consecutive days.



using $\beta = 0.09 \text{ K}^{-1}$. However, the model results did not match the measurement data. To improve the model, a unique β value was calculated using eqn (6) with the measurement data from the temperature cycle for each BVOC emitted by both spruce 1 and spruce 2. These unique β values were then used to calculate the pool standardised emission flux for each BVOC at 30 °C. The standardised emission flux and β for each BVOC were subsequently used to model the BVOC emissions during the daily cycle for spruce 1 and spruce 2.

For spruce 1, the model was only capable of reproducing measurements recorded in the dark (Fig. 8a). Data acquired under illumination were significantly underestimated by the model for all BVOCs, particularly at the highest PPF setting. This was unexpected, especially for monoterpenes which are usually assumed to be emitted solely from storage pools⁴² and thus entirely temperature dependent with no PPF dependence.¹⁹ Although a previous study observed that monoterpene emissions may also depend on light due to a significant contribution of *de novo* emissions, for several boreal species (*Pinus sylvestris*, *Picea abies*, *Larix decidua* and *Betula pendula*).⁷⁵ The emission of isoprene from Sitka spruce has also been shown to be temperature and PPF dependent,³² as it is emitted *via* a biosynthetic pathway, and therefore was not expected to be reproduced with the pooled emission model. The inability of the model to replicate the daily cycle measurements indicates that the biosynthetic pathway plays a role in the emission process for all BVOCs emitted by spruce 1 (Table S8†).

The emission profiles of six spruce 2 BVOCs including, C₆H₁₀O and C₂₀H₂₄, were completely described by the pooled emission model (Fig. 8b and Table S9†). For the remaining BVOCs the pooled model was unable to completely reproduce the measured data, indicating that biosynthetic pathways contributed to the emissions from spruce 2 also. Among the sixteen BVOCs common to the emissions of spruce 1 and spruce 2, there was a large difference between the extent to which the pooled emission model could reproduce the measured data. For example, 35% of the total emission flux of piperitone from spruce 1 could be reproduced using the pooled emission model, while for spruce 2 it accounted for 83% of the piperitone emission flux. The lower higher contribution of biosynthetic emissions (or higher contribution of pooled emissions) in spruce 2 is likely due to a lower photosynthesis rate, which was inferred from the CO₂ flux measurements.

3.5.1.2 Biosynthetic emission model. The biosynthetic emission model was much better than the pooled emission model at reproducing the spruce 1 emissions for the daily cycle and more accurately described the BVOC emissions under illumination (Fig. 8a). In total the biosynthetic model was able to completely reproduce the daily cycle emission profiles of 11 BVOCs emitted by spruce 1, including isoprene (Fig. S12†). This included five of the six BVOCs that produced post-illumination spikes. Emissions for the remaining BVOCs emitted by spruce 1 during the daily cycle could not be completely described by the

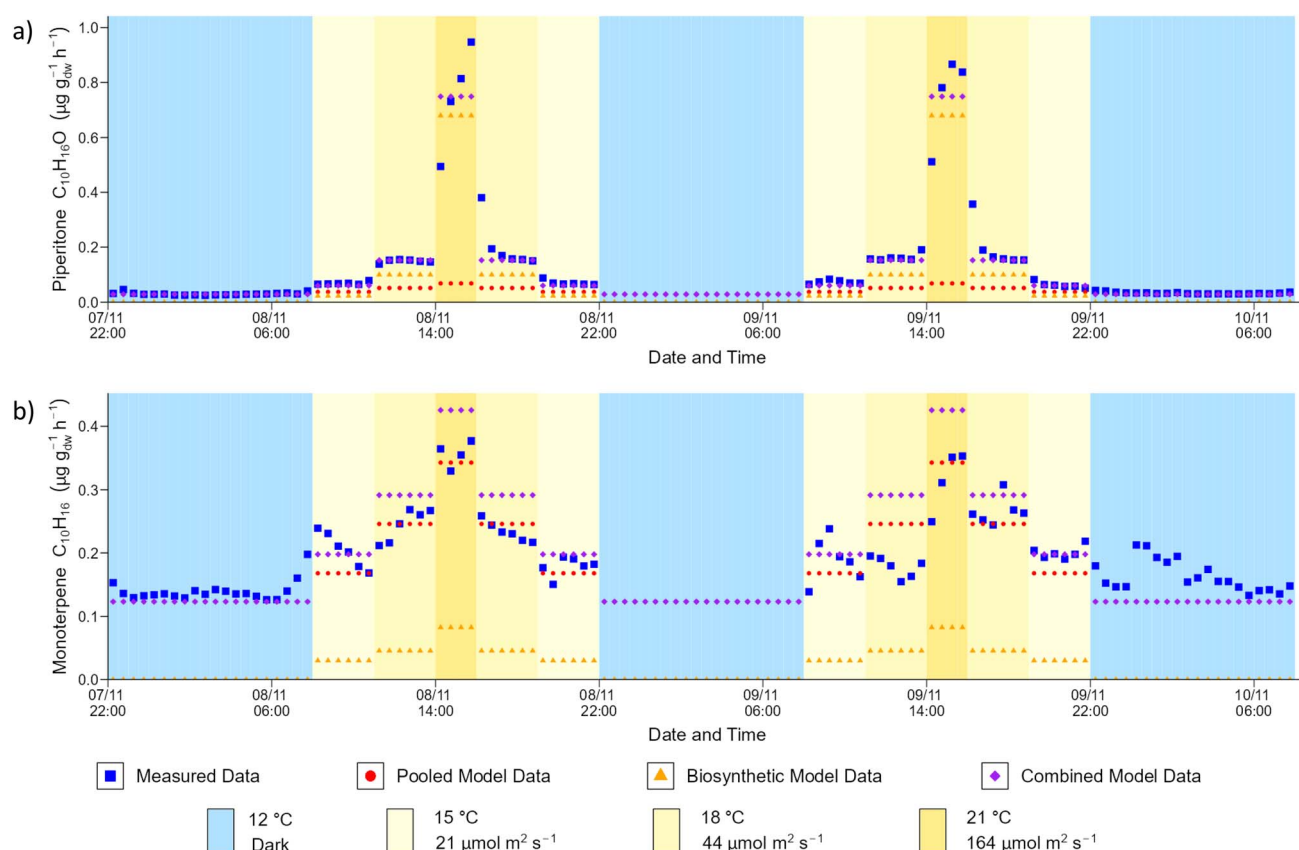


Fig. 8 Measured and all modelled data for (a) the emission of piperitone from spruce 1 and (b) the sum of monoterpenes from spruce 2.



biosynthetic model, indicating that these BVOCs were also originating from storage pools.

The contribution of the biosynthetic emission pathway to BVOC emissions from spruce 2 during the daily cycle was low. In the case of monoterpenes, this pathway only accounted for around 20% of the measured flux (Fig. 8b). Previous studies involving Sitka spruce have not reported a biosynthetic factor in monoterpene emissions,¹⁹ but it has been previously observed for beech¹⁴ and holm oak.⁶⁰ The low contribution of this pathway to spruce 2 compared to spruce 1 emissions is likely due to inhibition of the biosynthetic pathways, as evidenced by the lower photosynthetic activity of spruce 2 compared to spruce 1. This may explain why isoprene, which originates from the biosynthetic pathway, was not detected in the emissions from spruce 2, and why six of the spruce 2 BVOCs were completely replicated by the pooled emission model (Table S9†).

3.5.1.3 Combined emission model. The emission fluxes of eleven BVOCs from spruce 1 and six BVOCs from spruce 2 were completely reproduced using the biosynthetic emission model and pooled emission model, respectively. All other BVOCs had contributions from both emission pathways. A combined biosynthesis and pooled emission standardisation equation developed by Schuh *et al.* (1997)¹⁴ (eqn (7)) was therefore used to standardise and model the emissions of these BVOCs.

In total, the emission fluxes for 23 BVOCs emitted from spruce 1 were reproduced by the combined emission model. The contribution of each pathway to the total emission was BVOC dependent, although for all BVOCs the contribution from the biosynthetic pathway was larger. The combined emission model was able to accurately describe the remaining 26 BVOC emissions from spruce 2, including the sum of monoterpenes. This is the first time that the combined emission pathway has been used to standardise the emissions of Sitka spruce as previous studies used only the pooled emission model for monoterpenes,¹⁹ or biosynthetic model for isoprene.¹⁸

The combined emission pathway has been used previously to describe the emissions from sunflower and beech¹⁴ as well as Norway spruce.⁷⁶

The combined emission equation was used to standardise 13 of the 16 emissions common to both spruce saplings. The remaining three BVOCs: C₉H₈O, C₁₀H₁₄O₂ and C₂₀H₂₄, originated from different pathways in each sapling. The emission of C₉H₈O, identified as *E*-cinnamaldehyde, from spruce 1

originated from a biosynthetic pathway, while from spruce 2 it appeared as a pooled emission. For C₁₀H₁₄O₂ and C₂₀H₂₄ the emission from spruce 1 was *via* both pathways, while for spruce 2 the emission was *via* the pooled pathway only. This is consistent with other observations which suggest that both pathways are open for a healthy sapling (spruce 1), but the biosynthetic emission pathway is reduced for spruce 2 and the dominant emission pathway is diffusion from storage pools.

3.5.2 Standardisation application. The modelling approach which best replicated the daily cycle BVOC emissions for each sapling was used to provide the standardised emission flux at 1000 $\mu\text{mol m}^{-2} \text{s}^{-1}$ and 30 °C. The standardised emission rates for spruce 1 and spruce 2 are presented in Tables S8 and S9† respectively.

Piperitone was the dominant BVOC emitted by spruce 1, with a standardised emission flux of 17.29 $\mu\text{g g}_{\text{dw}}^{-1} \text{h}^{-1}$. Although piperitone has been detected in the emissions of Sitka spruce previously, an emission flux was not provided.³³ The standardised emission flux of isoprene from spruce 1 was 6.3 $\mu\text{g g}_{\text{dw}}^{-1} \text{h}^{-1}$, which is within the range of previously reported values determined under a variety of environmental conditions (Table 1).

The standardised emission fluxes for most BVOCs emitted by spruce 2 were lower than those for spruce 1, likely due to the lower photosynthesis rate which reduced the effectiveness of the biosynthetic emission pathway. However, the standardised total monoterpene emission flux from spruce 2 was 1.2 $\mu\text{g g}_{\text{dw}}^{-1} \text{h}^{-1}$, higher than the flux determined for spruce 1.

The emission flux data obtained for piperitone, isoprene and the sum of monoterpenes from spruce 1, have been scaled up to provide an estimate of the annual emission fluxes for these BVOCs, based on environmental conditions (air temperature and solar radiation) in Ireland.

Interestingly, the annual emission of isoprene (2080 $\mu\text{g g}^{-1} \text{year}^{-1}$) is greater than the annual emission for piperitone (1107 $\mu\text{g g}^{-1} \text{year}^{-1}$), despite piperitone being identified as the dominant emission in this work and having a standardised emission flux almost three times that of isoprene. This is due to the relationships between temperature, PPFD and BVOC emission, which are different for piperitone and isoprene (Fig. 9).

BVOC emission fluxes have an exponential relationship with temperature, and above a certain temperature, there is an inflection point where the emission flux increases significantly with increasing temperature. As shown in Fig. 9, piperitone

Table 1 Reported emission fluxes for isoprene and monoterpenes from Sitka spruce

Isoprene ($\mu\text{g g}_{\text{dw}}^{-1} \text{h}^{-1}$)	Monoterpene ($\mu\text{g g}_{\text{dw}}^{-1} \text{h}^{-1}$)	Temperature (°C)	PPFD ($\mu\text{mol m}^{-2} \text{s}^{-1}$)	Reference
3.06	0.95	28	1000	Evans <i>et al.</i> (1982) ⁷⁷
5.21	2.30	38	1000	Evans <i>et al.</i> ³²
0.05	1.50	16	360	Street <i>et al.</i> (1993) ⁷⁸
1–5	0.001–0.005	21–36	Not reported	Street <i>et al.</i> ¹⁸
14–17	—	28	230	Hayward <i>et al.</i> (2002) ⁷⁹
13.4	2.97	30	1000	Hayward <i>et al.</i> ^a ¹⁹
6.3	0.93	30	1000	This work ^a

^a Emission fluxes standardised, otherwise reported at measured conditions.



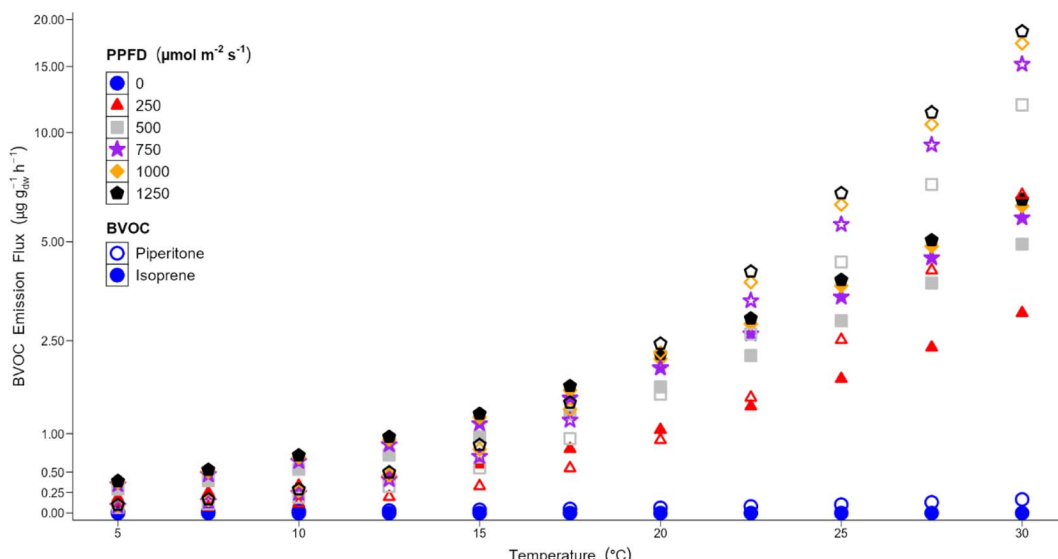


Fig. 9 Relationships between piperitone and isoprene emission fluxes with temperature at different PPFD values. Colour and shape indicate different PPFD, open symbols – piperitone, closed symbols – isoprene.

(open symbols) has a strong exponential relationship with temperature, with an inflection point around 15 °C. Below this temperature, the emission is quite low and there is little change in piperitone emission with temperature. Isoprene (closed symbols) has a much weaker relationship with temperature than piperitone, with an inflection point at around 22.5 °C, although it is not as clearly defined as it is for piperitone.

The emission fluxes for both BVOCs have a logarithmic relationship with PPFD. At a given temperature, the increase in emission flux decreases with fixed successive increases in PPFD, until a saturation point is reached. Below 750 $\mu\text{mol m}^{-2} \text{s}^{-1}$ the piperitone emission flux is strongly PPFD dependent. This relationship weakens as PPFD increases and the emission flux approaches the saturation point. The isoprene emission flux has a stronger relationship at lower PPFD than piperitone. This is seen in Fig. 9 through the sharp increase in emission flux between 0 and 250 $\mu\text{mol m}^{-2} \text{s}^{-1}$. The saturation point for isoprene is lower than for piperitone. The change in isoprene emission flux above 500 $\mu\text{mol m}^{-2} \text{s}^{-1}$ is significantly less than at lower PPFD values.

The exponential temperature and logarithmic PPFD relationships operate simultaneously. At lower temperatures, the influence of PPFD is stronger than that of temperature for both BVOCs. Above the respective inflection points, temperature plays a greater role in the emission flux. The emission flux of piperitone is less than that for isoprene at lower temperatures because of the strong exponential relationship between the piperitone emission flux and temperature. Isoprene has a more muted relationship with temperature and the emission flux is not as sensitive to lower temperatures. In the lower temperature regime the emission of isoprene is higher than piperitone, at all PPFD levels.

Typical temperatures for Ireland range between 6 °C and 17 °C. Under these conditions the emission of isoprene is higher than piperitone. The temperature for standardising BVOC emissions is 30 °C. At this temperature the emission of

piperitone is higher than isoprene. The conditions employed during the measurement cycles in this work fall between these two extremes and favour the emission of piperitone. Analysis of the temperature and PPFD dependence of these BVOC emissions explains why the annual emission flux of isoprene is greater than that for piperitone. The predicted increase in surface temperatures due to climate change,⁸⁰ would be sufficient to alter the piperitone-isoprene emission ratio from Sitka spruce in favour of piperitone. Therefore, under current future climate warming projections, piperitone would be the dominant BVOC emitted by Sitka spruce.

4. Conclusions

Using a novel combination of online and offline instrumentation, Sitka spruce saplings were found to emit 74 BVOCs under different controlled light and temperature conditions in a plant growth chamber. The BVOC emissions were dominated by oxygenated VOCs containing one to five O atoms, which accounted for 70% of the detected compounds (52 oxygenated BVOCs). Previous studies identified less than ten BVOCs emitted by Sitka spruce and the results from this study therefore serve to highlight the effectiveness of the ToF-CIMS and TD-GC-MS combination for detecting both the high number and diversity of BVOCs emitted from vegetation.

Piperitone ($\text{C}_{10}\text{H}_{16}\text{O}$) was, for the first time, found to be the dominant emission, followed by isoprene (C_5H_8) and the sum of five monoterpenes, which included myrcene, β -phellandrene, δ -limonene, α -pinene, and camphene. All BVOC emissions showed the expected diurnal pattern, with maxima occurring when temperature and light were at their highest. Six of the BVOC emissions, including isoprene, experienced a post-illumination burst.

The dependence of the BVOC fluxes on temperature and PPFD was investigated using three different growth cycles and



the results used to determine the contribution of both biosynthetic and pooled emission pathways to Sitka spruce emissions for the first time. The vast majority of BVOCs were found to depend on both pathways, with only eleven emissions attributed solely to the biosynthetic pathway.

The majority of the BVOC emissions were standardised to a temperature of 30 °C and PPFD of 1000 $\mu\text{mol m}^{-2} \text{s}^{-1}$ using a combined biosynthetic and pooled emission model. The standardised emission factor for piperitone ($17.29 \mu\text{g g}_{\text{dw}}^{-1} \text{h}^{-1}$) was the highest, followed by isoprene ($6.3 \mu\text{g g}_{\text{dw}}^{-1} \text{h}^{-1}$) and monoterpenes ($0.93 \mu\text{g g}_{\text{dw}}^{-1} \text{h}^{-1}$). However, under temperature and light conditions typical for most Sitka spruce plantations, *e.g.*, in Ireland, the estimated annual emission flux for isoprene was in fact higher than that for piperitone, due to the complex relationship between temperature, PPFD and emission for these BVOCs. This highlights the importance of assessing BVOC emissions under conditions relevant to the local climate.

Data availability

Code and data are available at: 10.5281/zenodo.10514476. A data availability statement (DAS) is required to be submitted alongside all articles.

Author contributions

HF, JK, JW and AW designed the experiments, which were carried out by HF. IS, DM and KK performed TD-GC-MS analysis of samples and HF did all other analysis in consultation with JK, AW and JW. HF prepared the manuscript with contributions from all authors.

Conflicts of interest

The authors declare that they have no conflict of interest.

Acknowledgements

This work was funded by the Irish Environmental Protection Agency through an Irish Research Council, Government of Ireland Postgraduate Scholarship (GOIPG/2019/1189), by the European Union's Horizon 2020 research and innovation programme (EUROCHAMP-2020, grant no. 73097), the French government under the France 2030 investment plan through the French National Research Agency (ANR-22-CE22-0003-01). The authors would like to thank Dr Dean Venables from University College Cork for laboratory access.

References

- 1 C. Geron, R. Rasmussen, R. Arnts and A. Guenther, A review and synthesis of monoterpene speciation from forests in the United States, *Atmos. Environ.*, 2000, **34**(11), 1761–1781.
- 2 TEAGASC, *Forest Statistics Ireland*, 2023.
- 3 Forestry Statistics, *National Forest Inventory*, 2023.
- 4 C. J. O'Callaghan, S. Irwin, K. A. Byrne and J. O'Halloran, The role of planted forests in the provision of habitat: an Irish perspective, *Biodivers. Conserv.*, 2026, **26**, 3103–3124.
- 5 D. T. Williams, N. Straw, N. Fielding, M. Jukes and J. Price, The influence of forest management systems on the abundance and diversity of bark beetles (coleoptera: curculionidae: scolytinae) in commercial plantations of Sitka spruce, *For. Ecol. Manage.*, 2017, **398**, 196–207.
- 6 K. S. Carslaw, O. Boucher, D. V. Spracklen, G. W. Mann, J. G. L. Rae, S. Woodward, *et al.*, A review of natural aerosol interactions and feedbacks within the Earth system, *Atmos. Chem. Phys.*, 2010, **10**(4), 1701–1737.
- 7 M. Mahilang, M. K. Deb and S. Pervez, Biogenic secondary organic aerosols: a review on formation mechanism, analytical challenges and environmental impacts, *Chemosphere*, 2021, **262**, 127771.
- 8 M. Hallquist, J. C. Wenger, U. Baltensperger, Y. Rudich, D. Simpson, M. Claeys, *et al.*, The formation, properties and impact of secondary organic aerosol: current and emerging issues, *Atmos. Chem. Phys.*, 2009, **82**, 5155–5236.
- 9 M. Shrivastava, C. D. Cappa, J. Fan, A. H. Goldstein, A. B. Guenther, J. L. Jimenez, *et al.*, Recent advances in understanding secondary organic aerosol: implications for global climate forcing, *Rev. Geophys.*, 2017, **55**(2), 509–559.
- 10 A. B. Guenther, R. K. Monson and R. Fall, Isoprene and monoterpene emission rate variability: observations with eucalyptus and emission rate algorithm development, *J. Geophys. Res. Atmos.*, 1991, **96**(D6), 10799–10808.
- 11 D. T. Tingey, D. P. Turner, and J. A. Weber. Factors controlling the emissions of monoterpenes and other volatile organic compounds, in *Trace Gas Emissions by Plants*, Elsevier, 1991, pp. 93–119. Available from: <https://linkinghub.elsevier.com/retrieve/pii/B9780126390100500091>
- 12 A. B. Guenther, P. R. Zimmerman, P. C. Harley, R. K. Monson and R. Fall, Isoprene and monoterpene emission rate variability: model evaluations and sensitivity analyses, *J. Geophys. Res.*, 1993, **98**(D7), 12609.
- 13 J. Kesselmeier and M. Staudt, Biogenic volatile organic compounds (VOC): an overview on emission, physiology and ecology, *J. Atmos. Chem.*, 1999, **(33)**, 23–88.
- 14 G. Schuh, A. C. Heiden, T. H. Hoffmann, J. Kahl, P. Rockel, J. Rudolph, *et al.*, Emissions of volatile organic compounds from sunflower and beech: dependence on temperature and light intensity, *J. Atmos. Chem.*, 1997, **27**(3), 291–318.
- 15 J. Peñuelas, J. Llusià and B. S. Gimeno, Effects of ozone concentrations on biogenic volatile organic compounds emission in the Mediterranean region, *Environ. Pollut.*, 1999, **105**(1), 17–23.
- 16 A. O. Mofikoya, K. Miura, R. P. Ghimire, J. D. Blande, M. Kivimäenpää, T. Holopainen, *et al.*, Understorey rhododendron tomentosum and leaf trichome density affect mountain birch VOC emissions in the subarctic, *Sci. Rep.*, 2018, **8**(1), 13261.
- 17 H. Hakola, T. Laurila, V. Lindfors, H. Hellén, A. Gaman and J. Rinne, Variation of the VOC emission rates of birch species



during the growing season, *Boreal Environ. Res.*, 2021, **6**, 237–2349.

18 R. A. Street, S. C. Duckham and C. N. Hewitt, Laboratory and field studies of biogenic volatile organic compound emissions from Sitka spruce (*Picea sitchensis* Bong.) in the United Kingdom, *J. Geophys. Res. Atmos.*, 1996, **101**(D17), 22799–22806.

19 S. Hayward, A. Tani, S. M. Owen and C. N. Hewitt, Online analysis of volatile organic compound emissions from Sitka spruce (*Picea sitchensis*), *Tree Physiol.*, 2004, **24**(7), 721–728.

20 T. H. Bertram, J. R. Kimmel, T. A. Crisp, O. S. Ryder, R. L. N. Yatavelli, J. A. Thornton, *et al.*, A field-deployable, chemical ionization time-of-flight mass spectrometer, *Atmos. Meas. Tech.*, 2011, **4**(7), 1471–1479.

21 Y. Kim, S. W. Kim, S. C. Yoon, J. S. Park, J. H. Lim, J. Hong, *et al.*, Characteristics of formation and growth of atmospheric nanoparticles observed at four regional background sites in Korea, *Atmos. Res.*, 2016, **12**, 80–91.

22 M. Riva, P. Rantala, J. E. Krechmer, O. Peräkylä, Y. Zhang, L. Heikkinen, *et al.*, Evaluating the performance of five different chemical ionization techniques for detecting gaseous oxygenated organic species, *Atmos. Meas. Technol.*, 2019, **12**(4), 2403–2421.

23 Ü. Niinemets, Mild *versus* severe stress and BVOCS: thresholds, priming and consequences, *Trends Plant Sci.*, 2010, **15**(3), 145–153.

24 L. G. Gomez, B. Loubet, F. Lafouge, R. Ciuraru, S. Bsaibes, J. Kammer, *et al.*, Effect of senescence on biogenic volatile organic compound fluxes in wheat plants, *Atmos. Environ.*, 2021, **266**, 118665.

25 M. Staudt, R. Joffre and S. Rambal, How growth conditions affect the capacity of *Quercus ilex* leaves to emit monoterpenes, *New Phytol.*, 2003, **158**(1), 61–73.

26 H. Hellén, T. Tykkä, S. Schallhart, E. Stratigou, T. Salameh and M. Iturrate-Garcia, Measurements of C10–C15 biogenic volatile organic compounds (BVOCs) with sorbent tubes, *EGUphere*, 2023, 1–30.

27 B. H. Lee, F. D. Lopez-Hilfiker, C. Mohr, T. Kurtén, D. R. Worsnop and J. A. Thornton, An iodide-adduct high-resolution time-of-flight chemical-ionization mass spectrometer: application to atmospheric inorganic and organic compounds, *Environ. Sci. Technol.*, 2014, **48**(11), 6309–6317.

28 Y. Ji, L. G. Huey, D. J. Tanner, Y. R. Lee, P. R. Veres, J. A. Neuman, *et al.*, A vacuum ultraviolet ion source (VUV-IS) for iodide-chemical ionization mass spectrometry: a substitute for radioactive ion sources, *Atmos. Meas. Technol.*, 2020, 3683–3696, Available from: <https://www.atmos-meas-tech-discuss.net/amt-2020-13/>.

29 A. Lavi, M. P. Vermeuel, G. A. Novak and T. H. Bertram, The sensitivity of benzene cluster cation chemical ionization mass spectrometry to select biogenic terpenes, *Atmos. Meas. Tech.*, 2018, **11**(6), 3251–3262.

30 M. Breitenlechner, G. A. Novak, J. A. Neuman, A. W. Rollins and P. R. Veres, A versatile vacuum ultraviolet ion source for reduced pressure bipolar chemical ionization mass spectrometry, *Atmos. Meas. Tech.*, 2022, **15**(5), 1159–1169.

31 E. R. Ashu-Ayem, U. Nitschke, C. Monahan, J. Chen, S. B. Darby, P. D. Smith, *et al.*, Coastal iodine emissions. 1. Release of I₂ by *Laminaria digitata* in chamber experiments, *Environ. Sci. Technol.*, 2012, **46**(19), 10413–10421.

32 R. C. Evans, Interspecies variation in terpenoid emissions from engelmann and sitka spruce seedlings, *For. Sci.*, 1985, **31**, 132–142.

33 A. Tani, S. Hayward and C. N. Hewitt, Measurement of monoterpenes and related compounds by proton transfer reaction-mass spectrometry (PTR-MS), *Int. J. Mass Spectrom.*, 2003, 223–224, 561–578.

34 R. Janson, C. De Serves and R. Romero, Emission of isoprene and carbonyl compounds from a boreal forest and wetland in Sweden, *Agric. For. Meteorol.*, 1999, **98–99**, 671–681.

35 M. Portillo-Estrada and Ü. Niinemets, Massive release of volatile organic compounds due to leaf midrib wounding in *Populus tremula*, *Plant Ecol.*, 2018, **219**(9), 1021–1028.

36 J. Kesselmeier, L. Schäfer, P. Ciccioli, E. Brancaleoni, A. Cecinato, M. Frattoni, *et al.*, Emission of monoterpenes and isoprene from a Mediterranean oak species *Quercus ilex* L. measured within the BEMA (biogenic emissions in the mediterranean area) project, *Atmos. Environ.*, 1996, **30**(10–11), 1841–1850.

37 I. Filella, M. J. Wilkinson, J. Llusia and J. Peñuelas, Volatile organic compounds emissions in Norway spruce (*Picea abies*) in response to temperature changes – Filella – 2007 – Physiologia Plantarum – Wiley Online Library, *Physiol. Plant.*, 2007, **130**(1), 58–66.

38 K. R. Brown, W. A. Thompson and G. F. Weetman, Effects of N addition rates on the productivity of *Picea sitchensis*, *Thuja plicata*, and *Tsuga heterophylla* seedlings, *Trees*, 1996, **10**, 189–197.

39 I. J. Beverland, R. Milne, C. Boissard, D. H. ÓNéill, J. B. Moncrieff and C. N. Hewitt, Measurement of carbon dioxide and hydrocarbon fluxes from a Sitka Spruce forest using micrometeorological techniques, *J. Geophys. Res. Atmos.*, 1996, **101**(D17), 22807–22815.

40 G. Purser, J. Drewer, J. I. L. Morison and M. R. Heal, A first assessment of the sources of isoprene and monoterpene emissions from a short-rotation coppice *Eucalyptus gunnii* bioenergy plantation in the United Kingdom, *Atmos. Environ.*, 2021, **262**, 118617.

41 S. Haapanala, A. Ekberg, H. Hakola, V. Tarvainen, J. Rinne, H. Hellén, *et al.*, Mountain birch – potentially large source of sesquiterpenes into high latitude atmosphere, *Biogeosciences*, 2009, **6**(11), 2709–2718.

42 J. D. Fuentes, L. Gu, M. Lerdau, R. Atkinson, D. Baldocchi, J. W. Bottenheim, *et al.*, Biogenic hydrocarbons in the atmospheric boundary layer: a review, *Bull. Am. Meteorol. Soc.*, 2000, **81**(7), 1537–1575.

43 R. Seco, J. Peñuelas and I. Filella, Short-chain oxygenated VOCs: emission and uptake by plants and atmospheric sources, sinks, and concentrations, *Atmos. Environ.*, 2007, **41**(12), 2477–2499.



44 A. Scala, S. Allmann, R. Mirabella, M. Haring and R. Schuurink, Green leaf volatiles: a plant's multifunctional weapon against herbivores and pathogens, *Int. J. Mol. Sci.*, 2013, **14**(9), 17781–17811.

45 D. Helmig, J. Ortega, A. Guenther, J. D. Herrick and C. Geron, Sesquiterpene emissions from loblolly pine and their potential contribution to biogenic aerosol formation in the Southeastern US, *Atmos. Environ.*, 2006, **40**(22), 4150–4157.

46 H. Hakola, V. Tarvainen, J. Bäck, H. Ranta, B. Bonn, J. Rinne, *et al.*, Seasonal variation of mono- and sesquiterpene emission rates of Scots pine, *Biogeosciences*, 2006, **3**(1), 93–101.

47 A. P. Praplan, S. Schobesberger, F. Bianchi, M. P. Rissanen, M. Ehn, T. Jokinen, *et al.*, Elemental composition and clustering behaviour of α -pinene oxidation products for different oxidation conditions, *Atmos. Chem. Phys.*, 2015, **15**(8), 4145–4159.

48 S. Kim, T. Karl, A. Guenther, G. Tyndall, J. Orlando, P. Harley, *et al.*, Emissions and ambient distributions of Biogenic Volatile Organic Compounds (BVOC) in a ponderosa pine ecosystem: interpretation of PTR-MS mass spectra, *Atmos. Chem. Phys.*, 2010, **13**, 1759–1771.

49 M. J. Kim, M. C. Zoerb, N. R. Campbell, K. J. Zimmermann, B. W. Blomquist, B. J. Huebert, *et al.*, Revisiting benzene cluster cations for the chemical ionization of dimethyl sulfide and select volatile organic compounds, *Atmos. Meas. Tech.*, 2016, **9**(4), 1473–1484.

50 T. M. VanReken, J. P. Greenberg, P. C. Harley, A. B. Guenther and J. N. Smith, Direct measurement of particle formation and growth from the oxidation of biogenic emissions, *Atmos. Chem. Phys.*, 2006, 4403–4413.

51 A. Ylisirniö, A. Buchholz, C. Mohr, Z. Li, L. Barreira, A. Lambe, *et al.*, Composition and volatility of secondary organic aerosol (SOA) formed from oxidation of real tree emissions compared to simplified volatile organic compound (VOC) systems, *Atmos. Chem. Phys.*, 2020, **20**(9), 5629–5644.

52 A. Kännaste, N. Vongvanich and A. K. Borg-Karlsson, Infestation by a Nalepella species induces emissions of α - and β -farnesenes, (–)-linalool and aromatic compounds in Norway spruce clones of different susceptibility to the large pine weevil, *Arthropod Plant Interact.*, 2008, **2**(1), 31–41.

53 D. Helmig, R. W. Daly, J. Milford and A. Guenther, Seasonal trends of biogenic terpene emissions, *Chemosphere*, 2013, **93**(1), 35–46.

54 B. F. Hrutfiord, S. M. Hopley and R. I. Gara, Monoterpenes in sitka spruce: within tree and seasonal variation, *Phytochemistry*, 1974, **13**(10), 2167–2170.

55 E. M. von Rudloff, Variation in leaf oil terpene composition of Sitka spruce, *Phytochemistry*, 1978, **17**(1), 127–130.

56 J. E. Brooks, J. H. Borden, H. D. Pierce Jr and G. R. Lister, Seasonal variation in foliar and bud monoterpenes in Sitka spruce, *Can. J. Bot.*, 1987, **65**(6), 1249–1252.

57 C. N. Hewitt and R. A. Street, A qualitative assessment of the emission of non-methane hydrocarbon compounds from the biosphere to the atmosphere in the U.K.: present knowledge and uncertainties, *Atmos. Environ. Part Gen. Top.*, 1992, **26**(17), 3069–3077.

58 E. Bourtsoukidis, J. Williams, J. Kesselmeier, S. Jacobi and B. Bonn, From emissions to ambient mixing ratios: online seasonal field measurements of volatile organic compounds over a Norway spruce-dominated forest in central Germany, *Atmos. Chem. Phys.*, 2014, **14**(13), 6495–6510.

59 K. Kempf, H. Westberg and C. Claiborn, Hydrocarbon emissions from spruce species using environmental chamber and branch enclosure methods, *Atmos. Environ.*, 1996, 1381–1389.

60 N. Lang-Yona, Y. Rudich, T. F. Mentel, A. Bohne, A. Buchholz, A. Kiendler-Scharr, *et al.*, The chemical and microphysical properties of secondary organic aerosols from Holm Oak emissions, *Atmos. Chem. Phys.*, 2010, **10**(15), 7253–7265.

61 H. Hakola, J. Rinne and T. Laurila, The hydrocarbon emission rates of tea-leaved willow (*Salix phylicifolia*), silver birch (*Betula pendula*) and European aspen (*Populus tremula*), *Atmos. Environ.*, 1998, **32**(10), 1825–1833.

62 E. Mäntylä, J. D. Blande and T. Klemola, Does application of methyl jasmonate to birch mimic herbivory and attract insectivorous birds in nature?, *Arthropod-Plant Interact.*, 2014, **8**(2), 143–153.

63 H. Hellén, A. P. Praplan, T. Tykkä, A. Helin, S. Schallhart, P. P. Schiestl-Aalto, *et al.*, Sesquiterpenes and oxygenated sesquiterpenes dominate the VOC (C_5 – C_{20}) emissions of downy birches, *Atmos. Chem. Phys.*, 2021, **21**(10), 8045–8066.

64 ThF. Mentel, E. Kleist, S. Andres, M. Dal Maso, T. Hohaus, A. Kiendler-Scharr, *et al.*, Secondary aerosol formation from stress-induced biogenic emissions and possible climate feedbacks, *Atmos. Chem. Phys.*, 2013, **13**(17), 8755–8770.

65 A. C. Heiden, T. Hoffmann, J. Kahl, D. Kley, D. Klockow, C. Langebartels, *et al.*, Emission of volatile organic compounds from ozone exposed plants, *Ecol. Appl.*, 1999, **9**(4), 8.

66 E. Bourtsoukidis, B. Bonn, A. Dittmann, H. Hakola, H. Hellén and S. Jacobi, Ozone stress as a driving force of sesquiterpene emissions: a suggested parameterisation, *Biogeosciences*, 2012, **9**(11), 4337–4352.

67 J. Laothawornkitkul, J. E. Taylor, N. D. Paul and C. N. Hewitt, Biogenic volatile organic compounds in the Earth system, *New Phytol.*, 2009, **183**(1), 27–51.

68 Z. Li, E. A. Ratliff and T. D. Sharkey, Effect of temperature on postillumination isoprene emission in oak and poplar, *Plant Physiol.*, 2011, **155**(2), 1037–1046.

69 N. C. Bouvier-Brown, G. W. Schade, L. Misson, A. Lee, M. McKay and A. H. Goldstein, Contributions of biogenic volatile organic compounds to net ecosystem carbon flux in a ponderosa pine plantation, *Atmos. Environ.*, 2012, **60**, 527–533.

70 T. Mochizuki, A. Tani, Y. Takahashi, N. Saigusa and M. Ueyama, Long-term measurement of terpenoid flux above a *Larix kaempferi* forest using a relaxed eddy accumulation method, *Atmos. Environ.*, 2014, **83**, 53–61.



71 M. Portillo-Estrada, T. Zenone, N. Arriga and R. Ceulemans, Contribution of volatile organic compound fluxes to the ecosystem carbon budget of a poplar short-rotation plantation, *GCB Bioenergy*, 2018, **10**(6), 405–414.

72 A. Tani and T. Mochizuki, Review: exchanges of volatile organic compounds between terrestrial ecosystems and the atmosphere, *J. Agric. Meteorol.*, 2021, **77**(1), 66–80.

73 M. A. Ibrahim, M. Maenpaa, V. Hassinen, S. Kontunen-Soppela, L. Malec, M. Rousi, *et al.*, Elevation of night-time temperature increases terpenoid emissions from *Betula pendula* and *Populus tremula*, *J. Exp. Bot.*, 2010, **61**(6), 1583–1595.

74 Y. Van Meeningen, G. Schurgers, R. Rinnan and T. Holst, Isoprenoid emission response to changing light conditions of English oak, European beech and Norway spruce, *Biogeosciences*, 2017, **14**(18), 4045–4060.

75 A. Ghirardo, K. Koch, R. Taipale, I. Zimmer, J. P. Schnitzler and J. Rinne, Determination of *de novo* and pool emissions of terpenes from four common boreal/alpine trees by $^{13}\text{CO}_2$ labelling and PTR-MS analysis, *Plant Cell Environ.*, 2010, **33**(5), 781–792.

76 T. Laurila, H. Hakola and V. Lindfors, Biogenic VOCs in continental Northern Europe—Concentrations and photochemistry, *Phys. Chem. Earth Part B Hydrol. Oceans Atmos.*, 1999, **24**(6), 689–693.

77 R. C. Evans, D. T. Tingey, M. L. Gumpertz and W. F. Burns, Estimates of isoprene and monoterpene emission rates in plants, *Bot. Gaz.*, 1982, **143**, 304–310.

78 R. Street, S. C. Duckham and C. N. Hewitt, Measurements of non-methane hydrocarbon emissions rates from Sitka spruce in the laboratory and field, *European Commission, Air Pollution Research Report 47: Joint Workshop CEC/BIATEX of 1030 EUROTRAC: General assessment of biogenic emissions and deposition of nitrogen compounds, sulphur compounds and oxidants in Europe*, 1993.

79 S. Hayward, C. N. Hewitt, J. H. Sartin and S. M. Owen, Performance characteristics and applications of a proton transfer reaction-mass spectrometer for measuring volatile organic compounds in ambient air, *Environ. Sci. Technol.*, 2002, **36**, 1554–1560.

80 IPCC, *Climate Change 2021: The Physical Science Basis. Contribution of Working Group I to the Sixth Assessment Report of the Intergovernmental Panel on Climate Change*, Cambridge University Press, Cambridge, UK, 2021. p. 3949.

